Adding the shape information to weak lensing peak statistics

Zuhui Fan
(SWIFAR, Yunnan University)

June 16, 2026
@non-Gaussian-Greece

Outline

- Introduction

- WL peak steepness statistics – adding the shape information
  - ❖ Simulation studies
  - ❖ First application using HSC data → baryonic feedback
  - ❖ Discussion

- Modeling the IA effects on WL high peak statistics
- Chinese Space Station Survey Telescope– CSST
- Summary

- **Introduction**

Among different probes, the weak lensing effect is uniquely important

Large-scale structures → bend the light rays gravitationally
Observables: tiny shape distortion and flux change → shear and magnification

Gravitational in origin → unique probe to study the dark side of the universe
dark matter and dark energy, law of gravity
Sensitive to both the cosmic expansion and the large scale structures

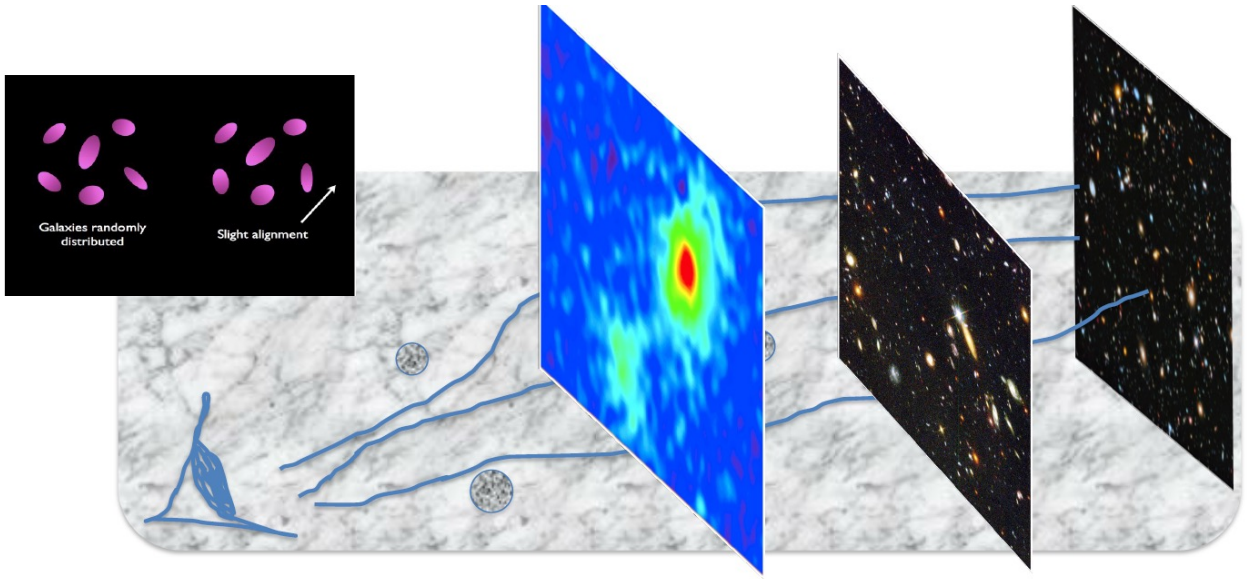

Nonlinear evolution → Phase coupling → Cosmic density field is non-Gaussian

Density field from simulation

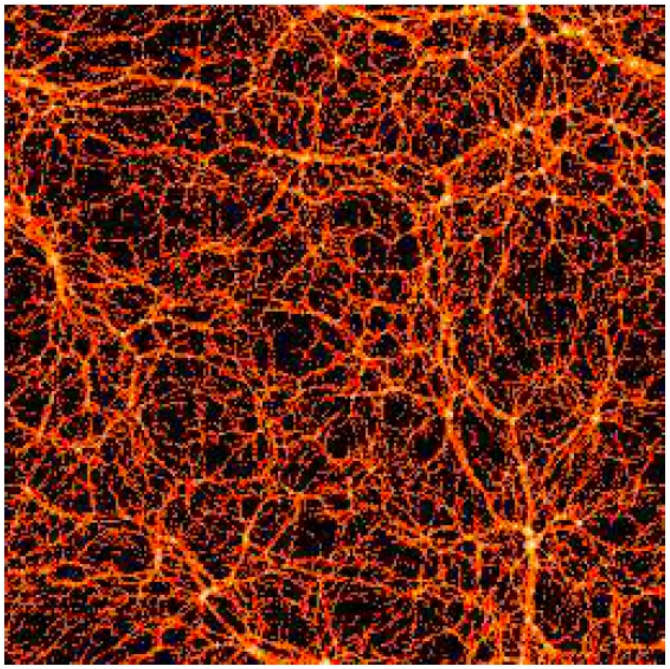

Phase-randomized field with same P(k)

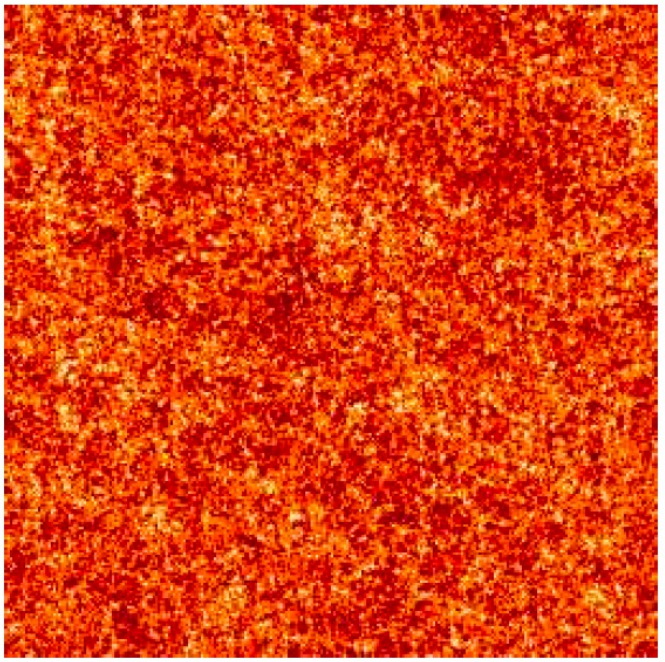

Coles & Chiang, 2000, Nature

Non-Gaussian statistics beyond 2pt are needed to fully reveal the cosmic information embedded in the large-scale structures

Non-Gaussian statistics are abundant

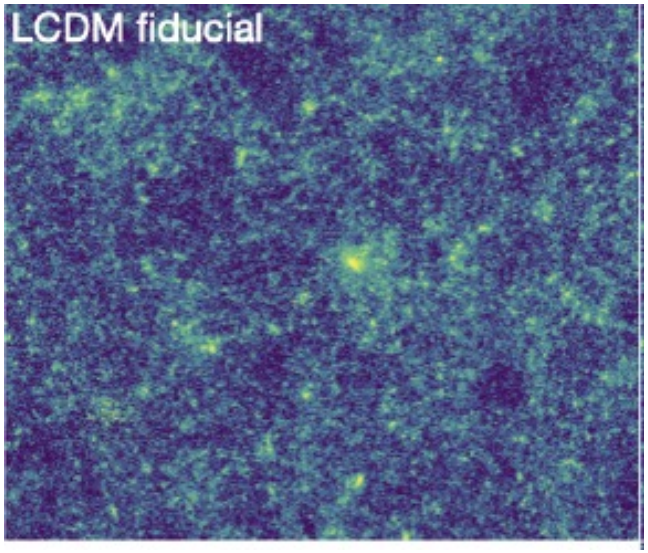

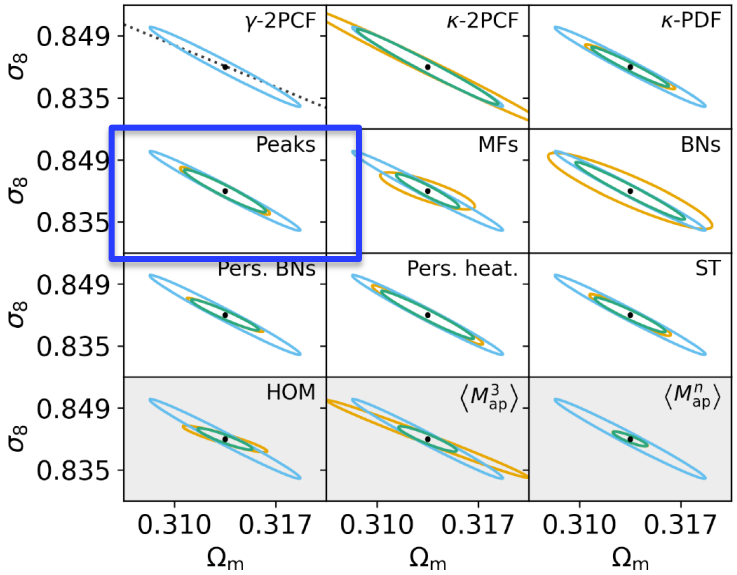

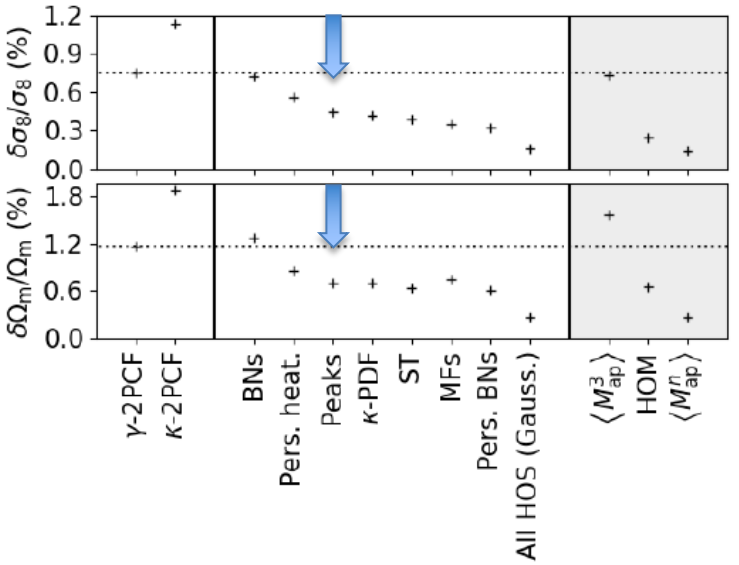

Euclid Collaboration HOWLS team et al. 2023

Weak lensing peak statistics have become a common non-Gaussian application

LOS matter concentrations (×lensing efficiency) → high WL signals → peaks in the WL mass maps → nonlinear and non-Gaussian features

By Z.W. Li

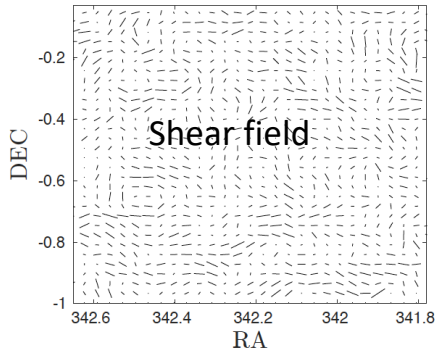

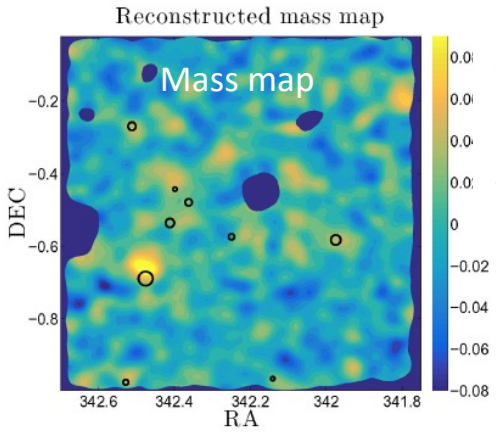

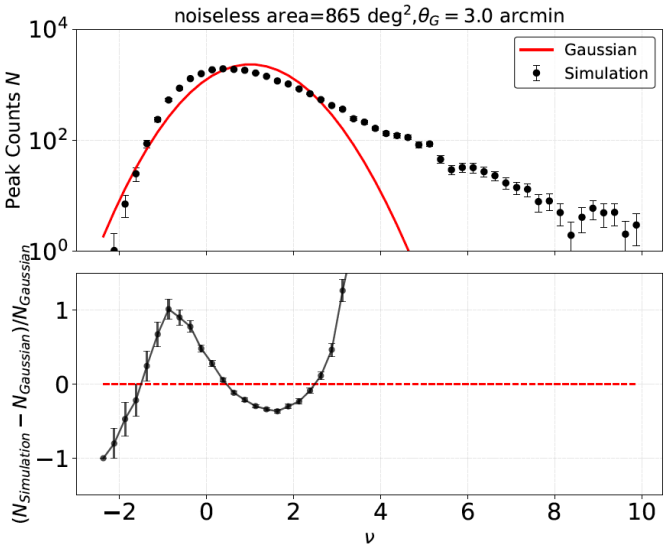

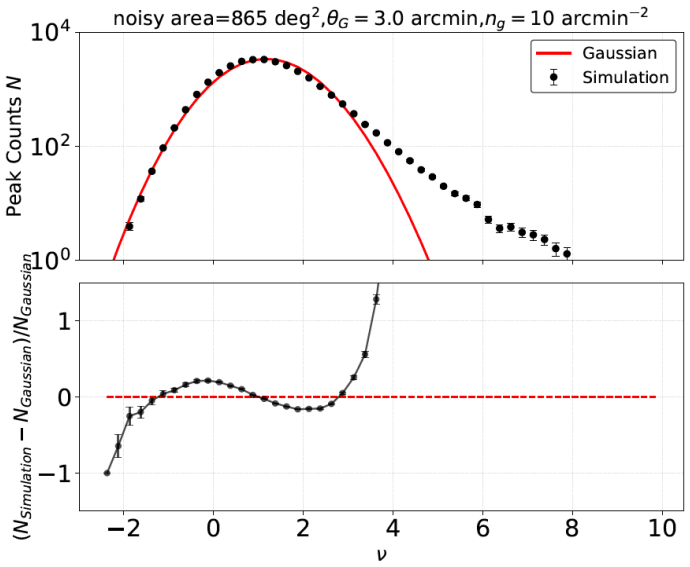

Significant excess over that of the Gaussian random field especially at the high peak end→ non-Gaussian information

Liu,X. et al. 2015

Peak statistics have been applied to different surveys (e.g., Liu,X. et al. 2015, Liu,J. et al. 2015, Liu, X. et al. 2016, Kacprzak et al. 2016, Martinet et al. 2018, Shan et al. 2018, Zurcher et al. 2022, Liu,X. et al. 2023, Harnois-Deraps et al. 2024)

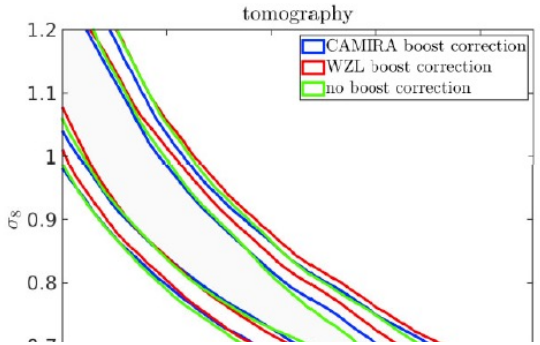

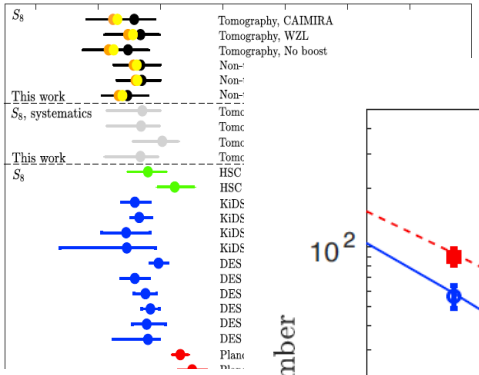

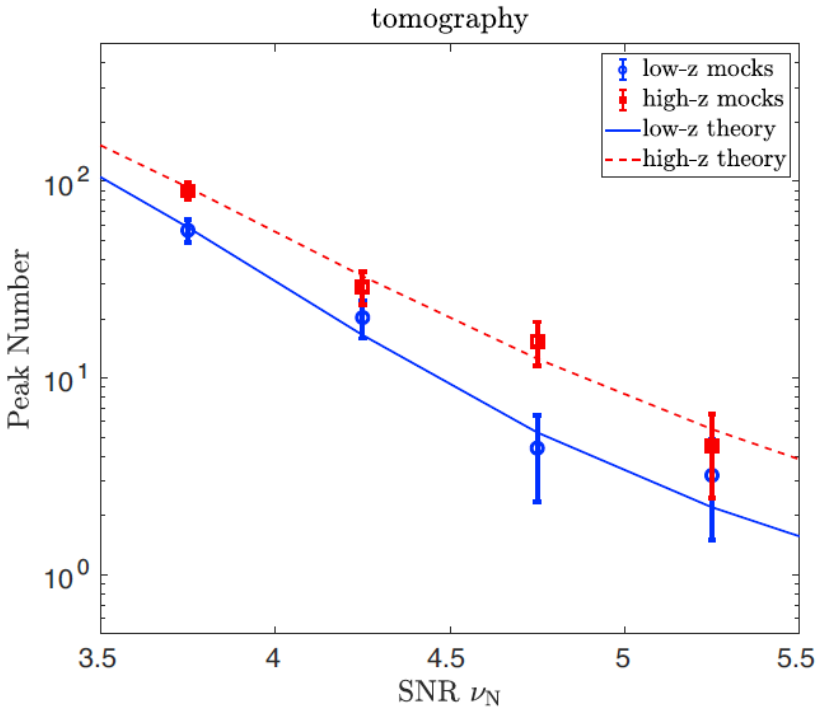

All the peak analyses are in terms of peak height distribution

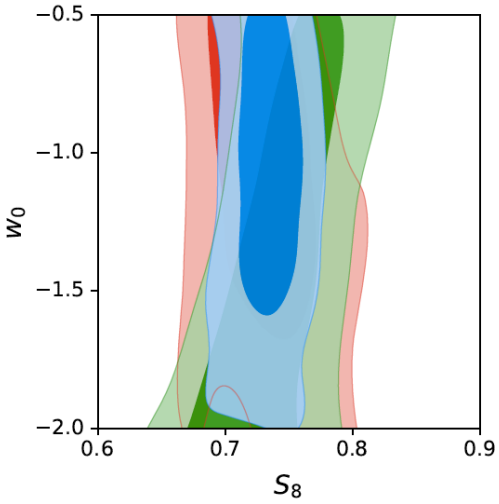

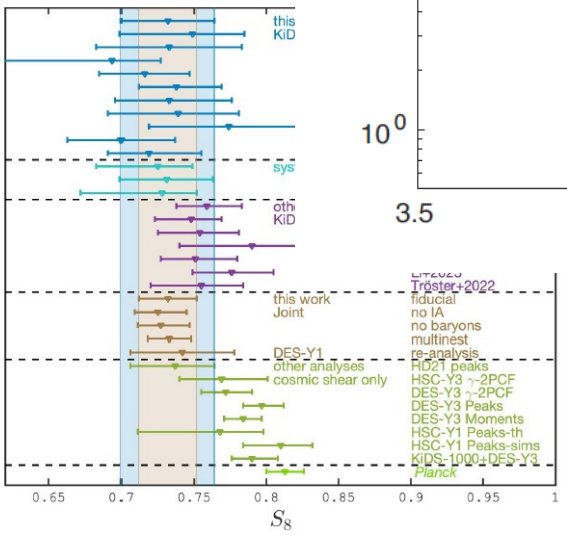

With deep learning, in Ribli et al. 2019, they analyzed the WL convergence map features, and found that the statistics of steepness (profile) of WL peaks carry additional cosmological information in comparison with the peak height statistics

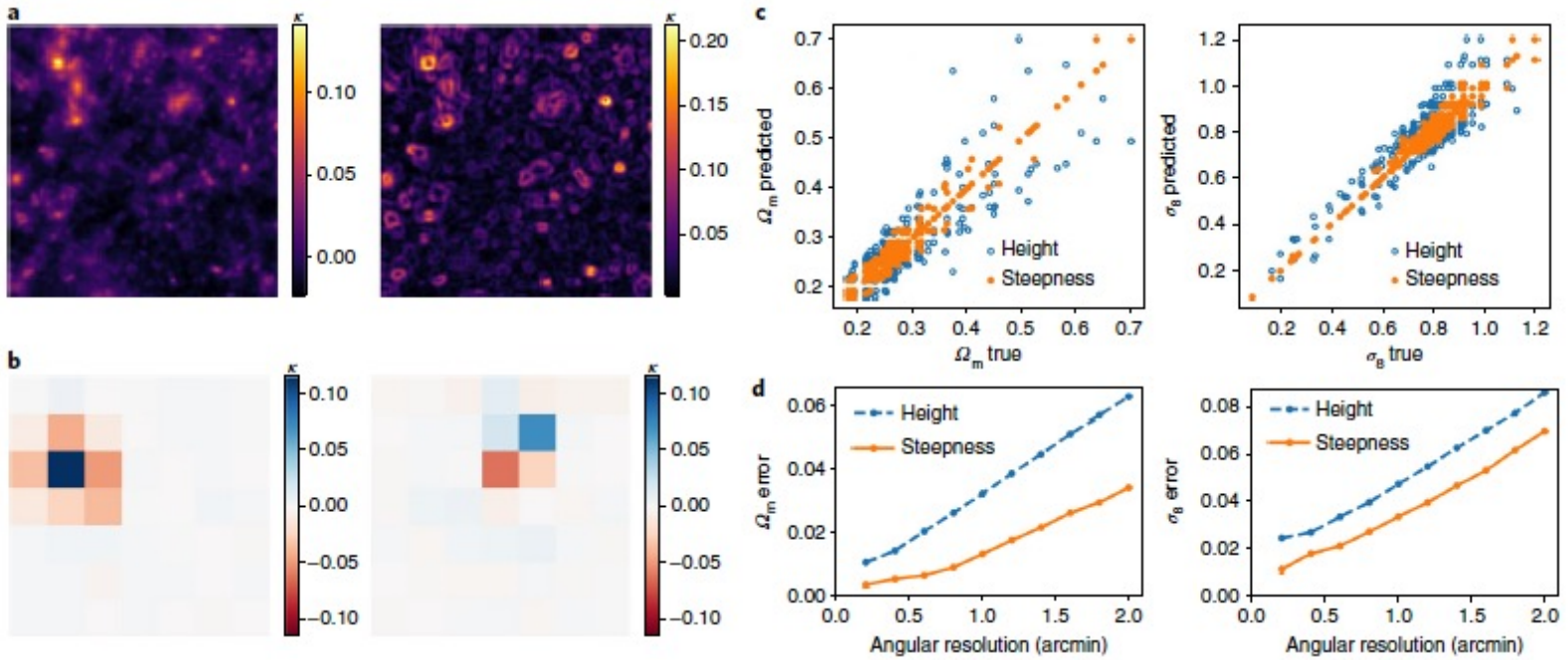

Laplace operator

$$L_1 = \frac{-10}{3}\begin{bmatrix} -0.05 & -0.2 & -0.05 \\ -0.2 & 1 & -0.2 \\ -0.05 & -0.2 & -0.05 \end{bmatrix},$$

$$L_2 = -4\begin{bmatrix} 0 & -0.25 & 0 \\ -0.25 & 1 & -0.25 \\ 0 & -0.25 & 0 \end{bmatrix}$$

Roberts cross kernels

$$R_x = \begin{bmatrix} 0 & 1 \\ -1 & 0 \end{bmatrix},$$

$$R_y = \begin{bmatrix} 1 & 0 \\ 0 & -1 \end{bmatrix},$$

$$G = \sqrt{G_x^2 + G_y^2},$$

Laplace operator → second derivative
Roberts cross kernels → first derivative

- **WL peak steepness statistics – adding the shape information**

❖ **Simulation studies and modeling (Li,Z.W. et al. 2023)**

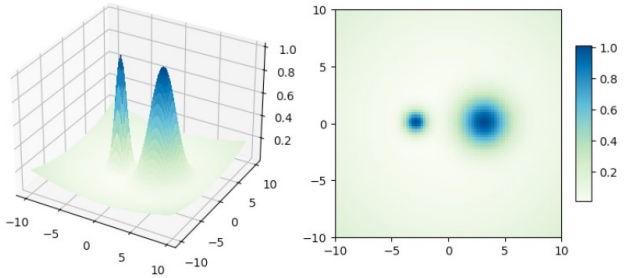

Mathematically, for a peak, its first derivatives are zero by definition. The steepness of a peak is reflected by its second derivatives

$$L_2 = -4\begin{bmatrix} 0 & -0.25 & 0 \\ -0.25 & 1 & -0.25 \\ 0 & -0.25 & 0 \end{bmatrix} \Longrightarrow \partial_{11}\mathrm{K} + \partial_{22}\mathrm{K}$$

With ray-tracing simulations, we perform analyses to compare the two statistics systematically
-- different noise levels and smoothing scales

In the Stage IV era → peak steepness statistics can indeed give better cosmological constraints

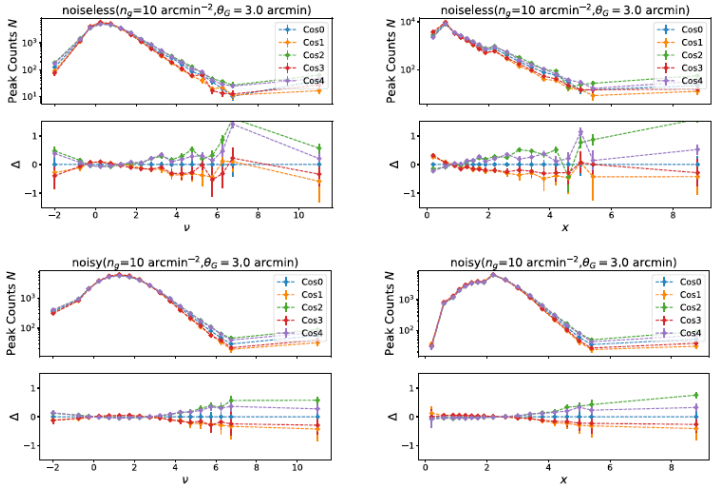

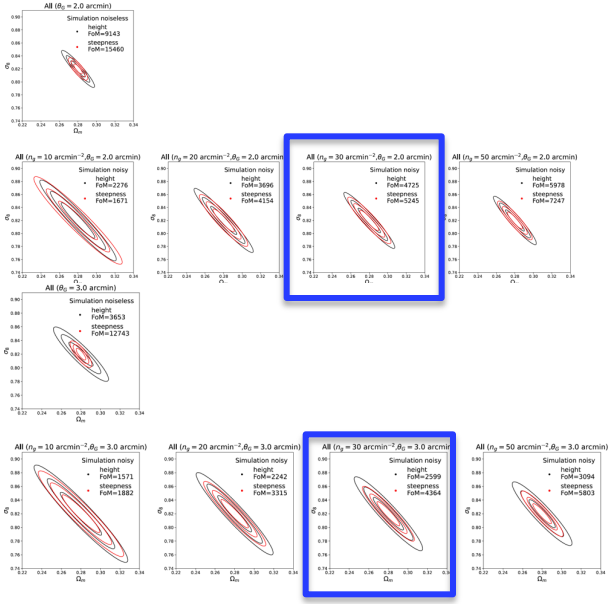

Steepness model for high peaks

(Li,Z.W. et al. 2023 , Fan,Z.H. et al. 2010, Yuan,S. et al. 2018)

Assumption: Single massive halos contribute dominantly to WL peaks ($M \geqq M_* \sim 10^{14} h^{-1} M_{sun}$)

→ valid for high peaks – **theoretically similar to cluster abundance, but different observables without the need to calibrate the mass-observable relation**

Including the shape noise and the LSS projection effects

→ adopt Gaussian approximation→ **forward modelling approach**

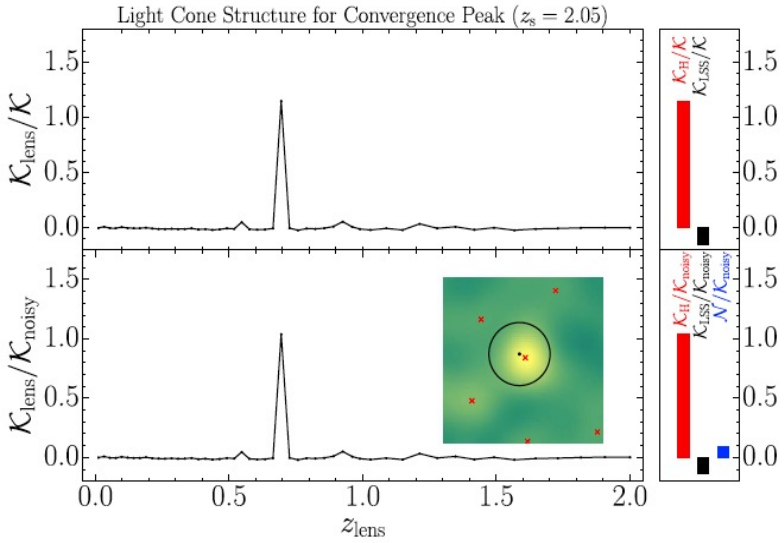

high peak

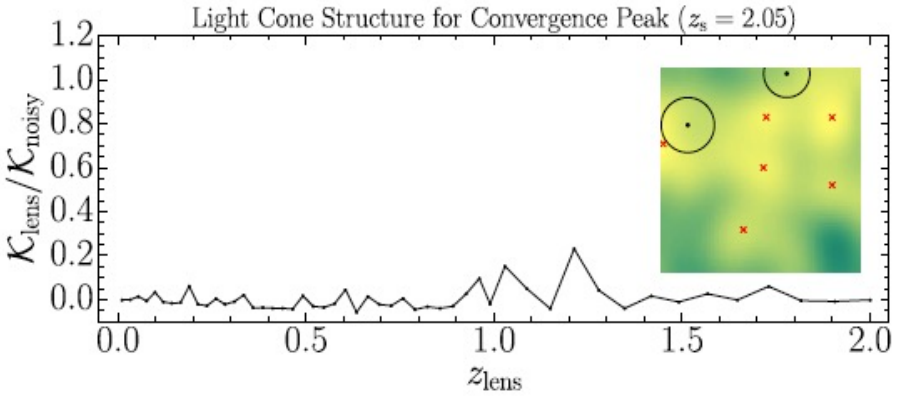

low peak

Steepness model for high peaks

(Li,Z.W. et al. 2023 , Fan,Z.H. et al. 2010, Yuan,S. et al. 2018)

→ adopt Gaussian approximation→ **forward modelling approach**

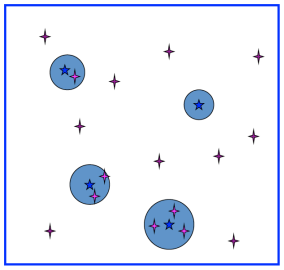

$$\mathcal{K} = \mathcal{K}_{\rm H} + \mathcal{K}_{\rm LSS} + \mathcal{N} \qquad n_{\rm peak}(y)dy = \left[n^{H}_{\rm peak}(y) + n^{N}_{\rm peak}(y)\right] dy$$

$$\hat{n}_{\rm peak}(\nu_N) = \exp\left[-\frac{(K_H^1)^2 + (K_H^2)^2}{\sigma_1^2}\right]\left\{\frac{1}{2\pi\theta_{N*}^2}\frac{1}{(2\pi)^{1/2}}\right\} \times \exp\left(-\frac{1}{2}u(\nu_N)^2\right) d\nu_N \int_0^\infty \frac{dx_N}{\left[2\pi\left(1-\gamma_N^2\right)\right]^{1/2}} \times \exp\left[-\frac{\left(m(x_N) - \gamma_N u(\nu_N)\right)^2}{2\left(1-\gamma_N^2\right)}\right] \times F(x_N)$$

$$\hat{n}_{\rm peak}(x_N)\Big|_{\nu_N \geq \nu_{\rm cut}} = \exp\left[-\frac{(K_H^1)^2 + (K_H^2)^2}{\sigma_1^2}\right]\left\{\frac{1}{(2\pi\theta_{N*})^2}\frac{(2\pi)^{1/2}}{2}\right\} \times \exp\left(-\frac{1}{2}m(x_N)^2\right) \times \mathrm{erfc}(t(\nu_{\rm cut}, x_N)) \times F(x_N)\, dx_N,$$

Physical ingredients: HMF, density profile, geometric distances

Incorporate systematics relatively straightforwardly: Baryonic effects→ halo profile, HMF, LSS

IA effects → lensing profile of clusters of galaxies, shape noise properties (Zhang et al. 2025)

The model works well for both height and steepness statistics for high peaks

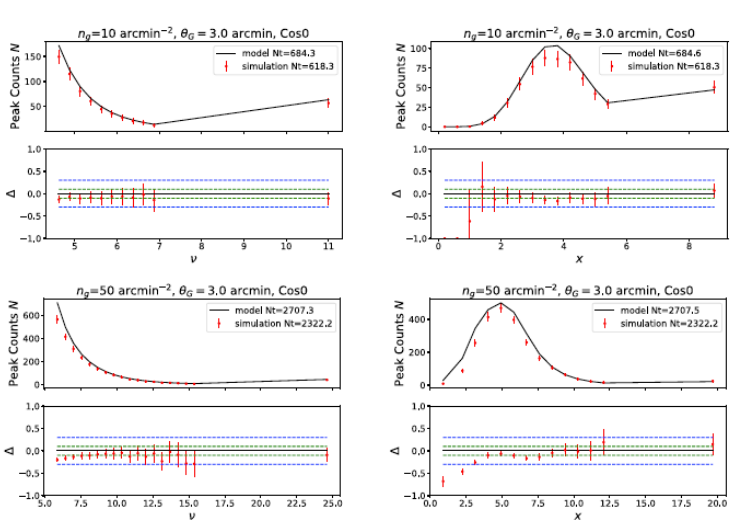

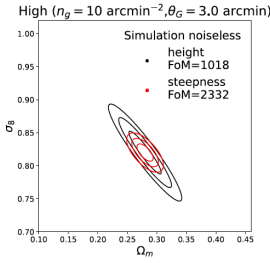

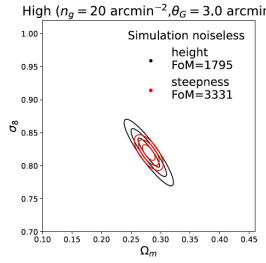

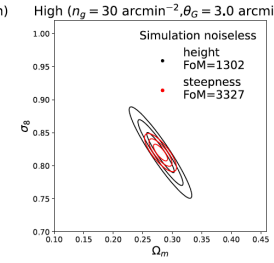

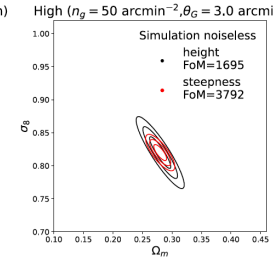

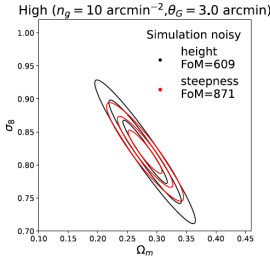

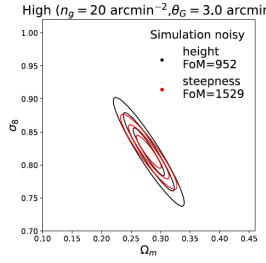

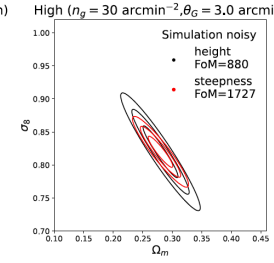

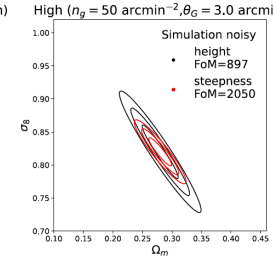

From the model, we can calculate the dependence of the two statistics on different physical parameters

Different sensitivities to the physical parameters (from our model)

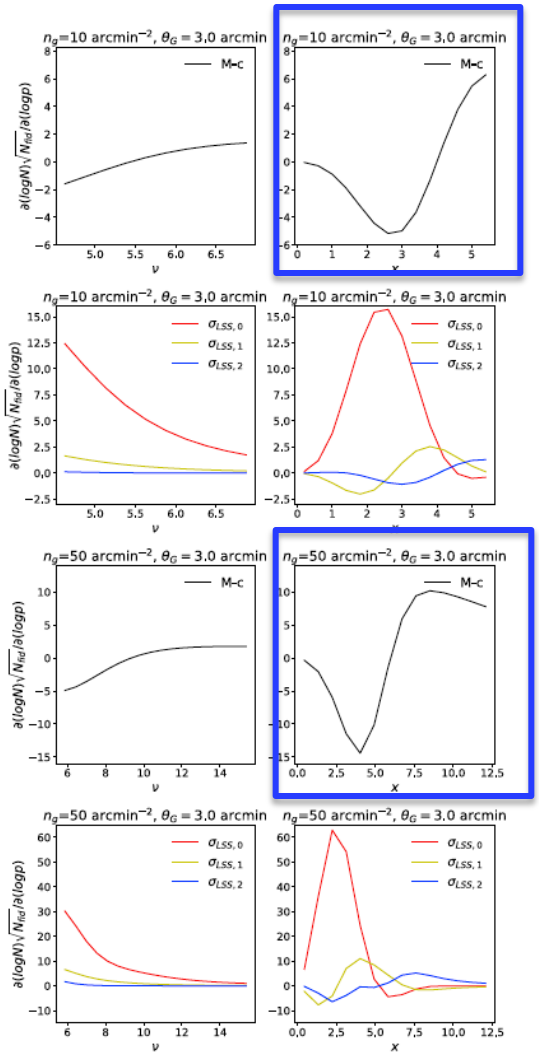

Steepness statistics:

$$c_{\rm vir} = \frac{A}{(1+z)^{0.71}} \left(\frac{M_{\rm vir}}{10^{14} h^{-1} {\rm M}_\odot} \right)^{-0.081}$$

More sensitive to halo profile (M-c)

-- M-c relation is mass and redshift dependent

-- different weight on halo mass function

More sensitive to LSS projection effects (cosmological info.)

In addition to cosmological constraints, steepness statistics can probe **the density profile of halos,** which encodes information of

-- the baryonic effects

-- dark matter properties

→ Unique advantage of peak steepness statistics

❖ First application of the WL peak steepness analyses to HSC S16A data

(Li, Z.W. et al. 2026)

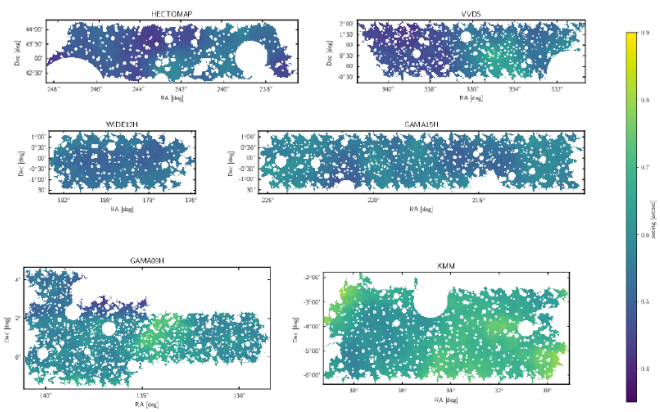

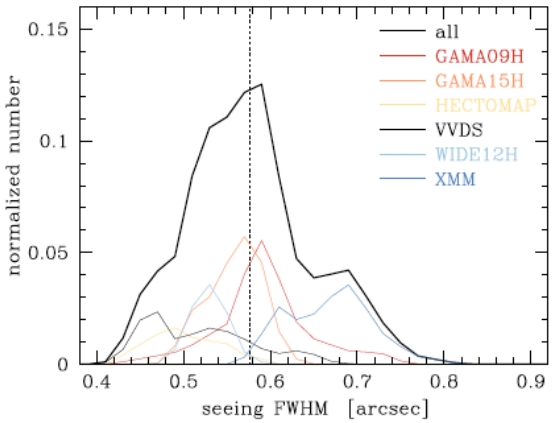

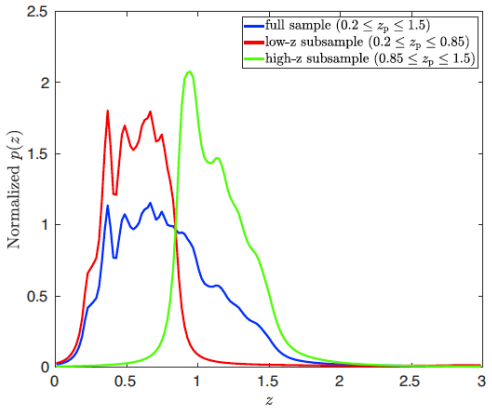

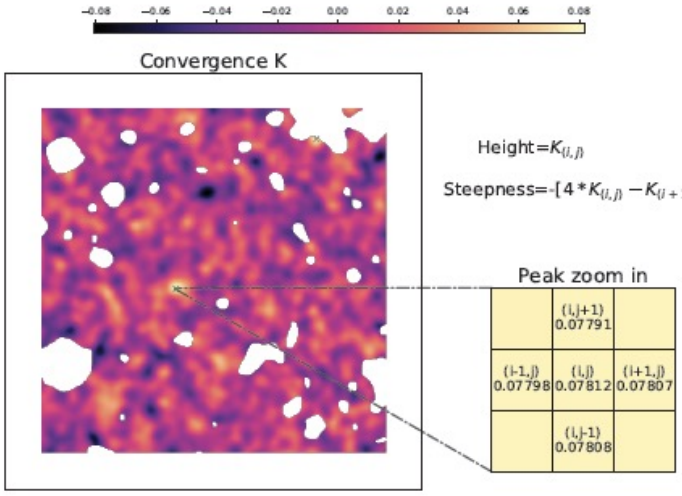

Number density ~18 armin^{-2}

Form shear field to convergence
-- smoothing scale 1.5 arcmin
-- corresponding shape noise $\boldsymbol{\sigma}_N$~0.018

Building filling factor maps from galaxy distribution → exclude areas with f<0.6 to mitigate the mask effects

Mock validation: Built mocks from N-body simultions with the same spatial and redshift distribution of sources – mask effects, convergence reconstrunction, dark matter halo properties, MCMC pipeline

→ using our peak model utilizing the HMcode-like approch to account for the baryonic effects reflected by the amplitude A of the mass-concentration relation of halos

Table 1. Priors.

Parameters	Flat prior ranges
$\Omega_{\rm m}$	$[0.05, 0.95]$
σ_8	$[0.20, 1.60]$
A	$[0.00, 10.00]$

$$c(M,z) = A\frac{1+z_{\rm f}}{1+z}$$

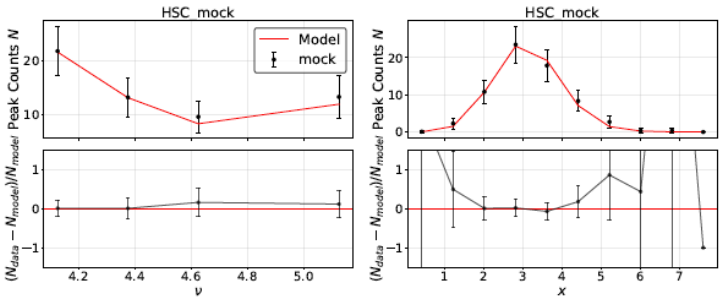

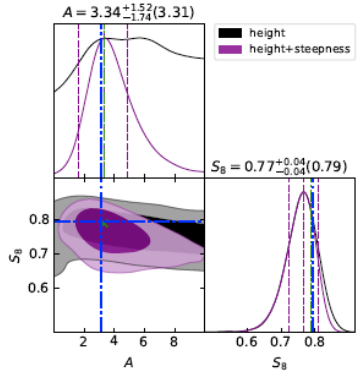

✓ Excellent agreements with the input cosmological parameters and A~3.34(3.31) well consistent with DM-only case of A=3.13 from HM2016

✓ By combining peak height and steepness analyses

Can indeed constrain M-c relation simultaneously with cosmological parameters

Potentially probe the baryonic effects from WL peak data only → control the induced bias and probe astrophysics

Observational results from HSC-SSP S16A

$S_8 = 0.76^{+0.08}_{-0.07}$ (MAP 0.79)

$A = 1.93^{+1.33}_{-1.16}$ (MAP 1.70)
(lower than that of the DM-only case)

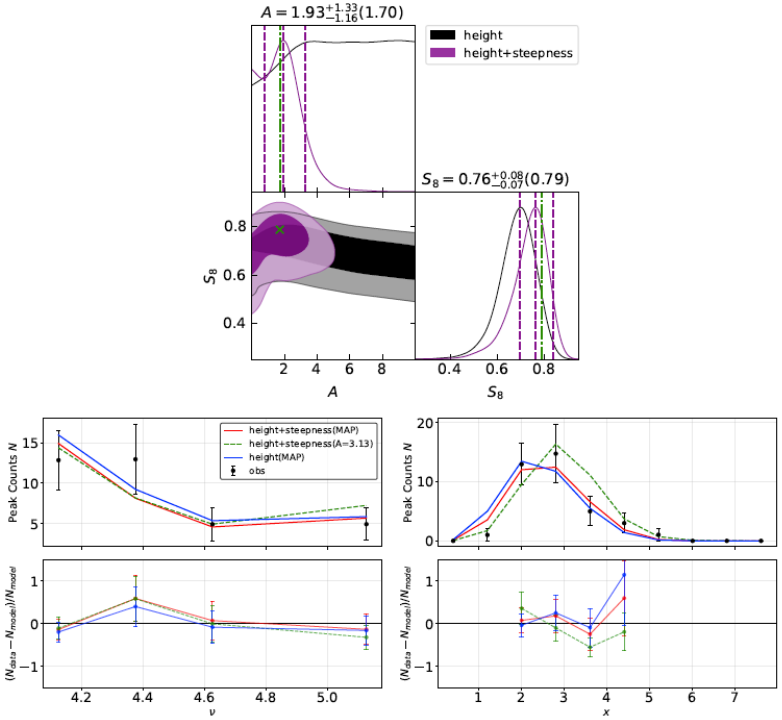

Comparing to the predictions with dark matter only ingredients (green dashed)

→ The observed steepness count distribution systematically shifts to lower values

→ The height distribution is not as sensitive to A as the steepness distribution

→ The advantage of adding the shape information to the peak analyses

The lower A → consistent with strong baryonic effects

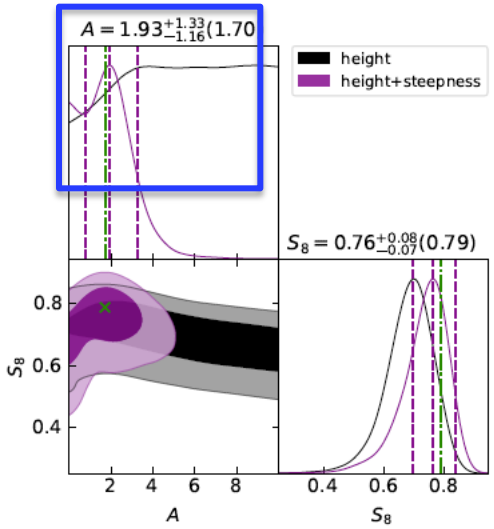

Mead et al. 2015, HMCode2016

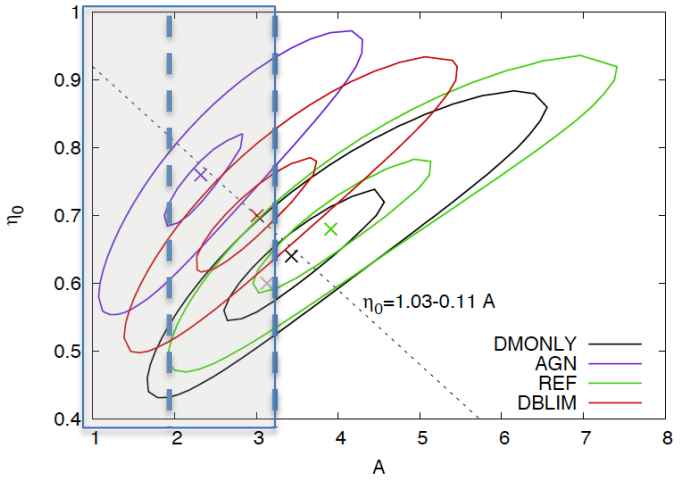

HSC Y3 3*2pt (Li,X.C. et al.2023)

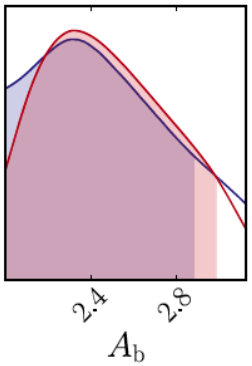

Applied the
tight prior of [2,3]

DES Y3 small-scale 2pt (Arico et al.2023), BCM

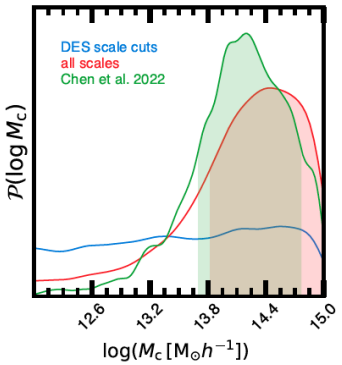

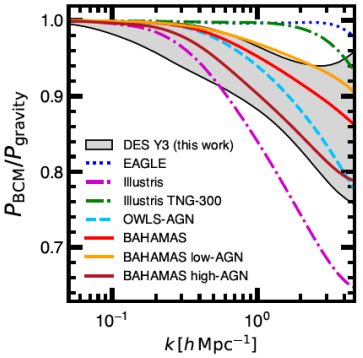

Our fiducial analysis models the baryonic feedback at small scales using HMCode 2016, and find a significant positive detection of baryonic feedback; $A_b = 2.34^{+0.40}_{-0.25}$,

Tests on different systematics

✓ B-mode test

B-mode peak height and steepness distributions are very much consistent with that of the pure noise maps – **No significant B-mode contanminations**

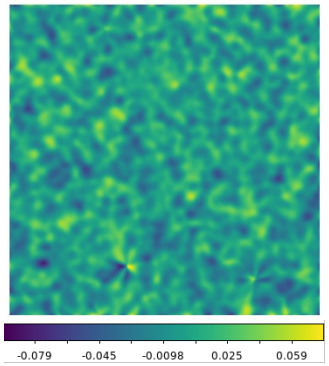

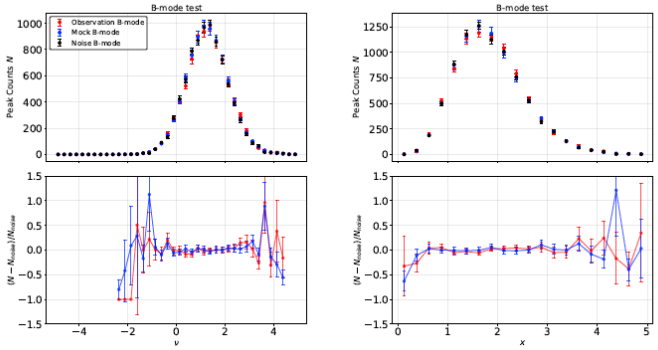

✓ Galaxy intrinsic alignments (IA contaminations)

Using simulations with IA settings (Zhang, T.Y. et al. 2022, 2025)

– **IA effects are much smaller than statistical uncertainties**

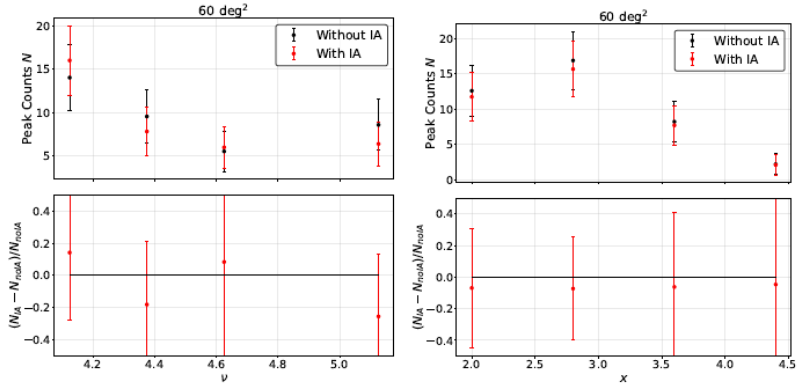

✓ Cluster member galaxy contaminations

Member galaxies in the shear sample dilute the lensing signals of their host clusters and decrease the local shape noise – **included in the model calculations**

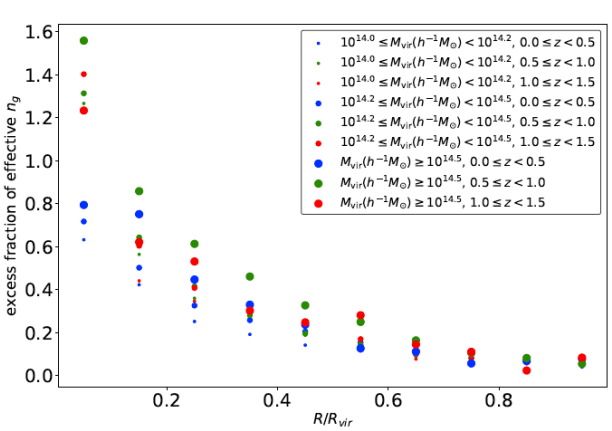

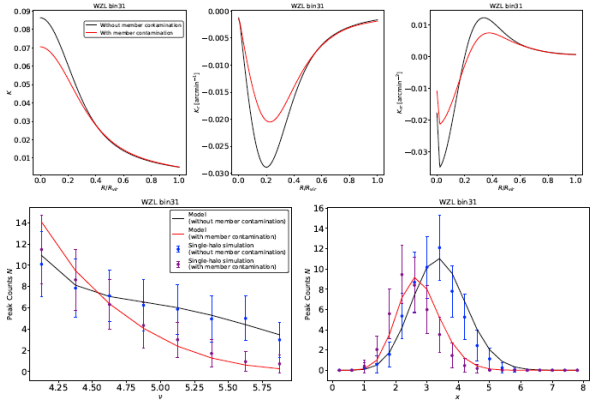

✓ Photo-z and shear measurements -- **insignificant** (Liu et al. 2023)

HSC S16A, shear measurement bias m~0.01

$\sigma[\Delta z_p/(1+ z_p)]$~0.05

❖ Discussion

- WL peak steepness analyses can provide sensitive constraints on halo profile → baryonic physics/dark matter properties
- Our first application to HSC data demonstrated well the feasibility in observational anlayses
- The lower A value from data is consistent with relatively strong bayonic feedback
- Potential to probe the physics of dark matter
- Very promising means in Stage IV WL survey analyses

- Our current analyses: contribute all bayonic effects to halo profile (like HMcode 2016 for power spectrum) → pointing to positive baryonic effects

- We are implementing the Baryon Correction Model (BCM) into the peak model (dark matter+gas+stellar, change halo mass and profile)
  → more physical information regarding baryonic feedback

- The effective area used in our analyse in ~60deg^2 → cosmic variance?

  We noticed the overlaps between some of the HSC S16A areas with eROSITA X-ray superclusters -- case studies

- Apply to HSC Y3

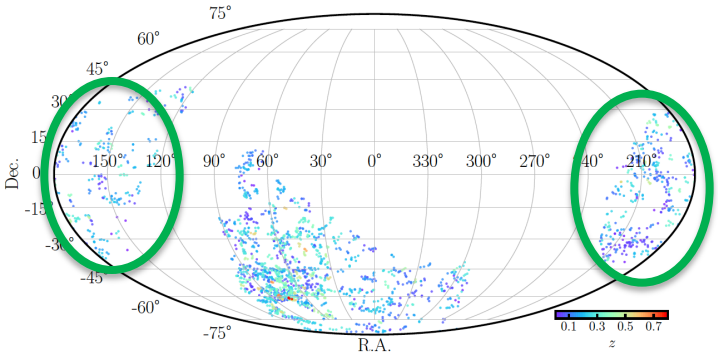

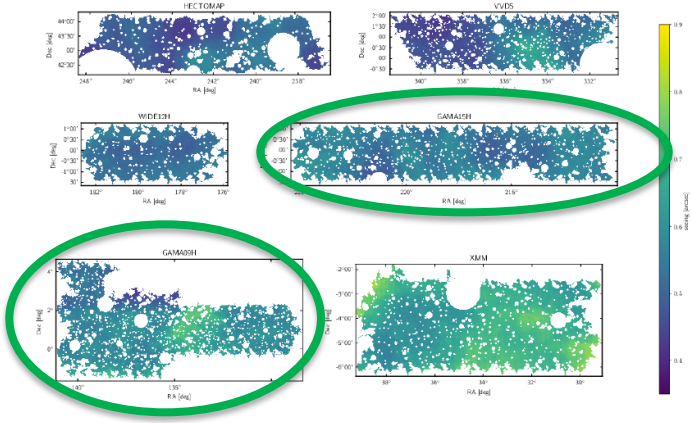

eRASS1 X-ray superclusters (Liu, A. et al.2024)

- **Modeling the IA effects on WL high peak statistics**

$$\gamma^{obs} = \gamma + \gamma^{I}$$

Galaxy intrinsic alignments are a major systematics in WL studies

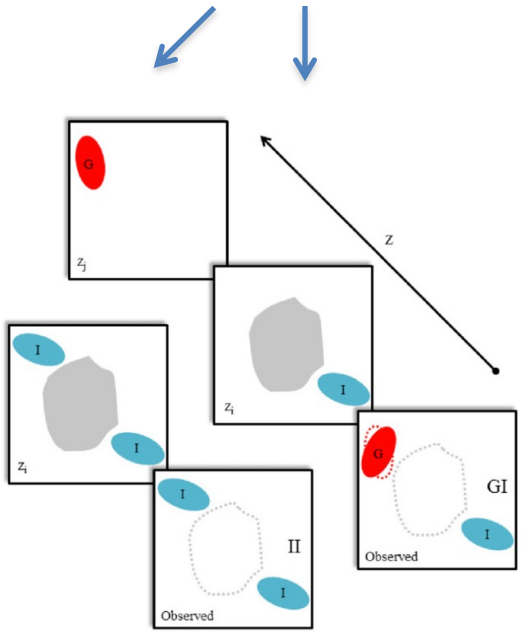

The IA effects on WL 2pt analyses have been studied systematically and extensively.

Their impacts on non-Gaussian statistics including WL peak statistics need to be investigated carefully

Harnois-Deraps et al. infusion approach （δ- NLA）

$$\epsilon_1^{\rm IA} = -\frac{A_{\rm IA}\bar{C}_1\bar{\rho}(z=0)}{D(z)}(s_{xx}-s_{yy}),$$

$$\epsilon_2^{\rm IA} = -\frac{2A_{\rm IA}\bar{C}_1\bar{\rho}(z=0)}{D(z)}s_{xy},$$

$$\epsilon_{1/2}^{\rm IA,\delta} = \epsilon_{1/2}^{\rm IA} \times (1 + b_{\rm TA}\delta)$$

Works well for relatively low peaks, and not accurate enough for high peaks where small-scale one-halo term is dominant (satellite galaxies) (e.g., Schneider & Bridle 2010, Kacprzak et al. 2016).

Simulation studies of IA impacts on WL peak statistics (Zhang et al. 2022, ApJ)

Using cosmological simulations with semi-analytical galaxy formation (Wei et al. 2018)

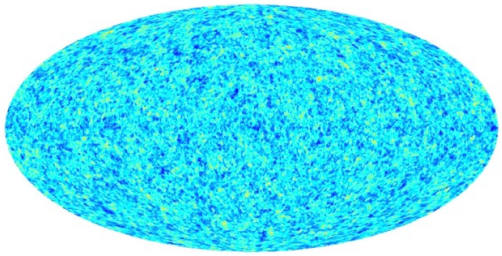

Central IA – given by the simulation
We change satellite IA to study their impacts on WL peaks

High-IA : radially aligned satellites
Low-IA: randomly orientated satellites

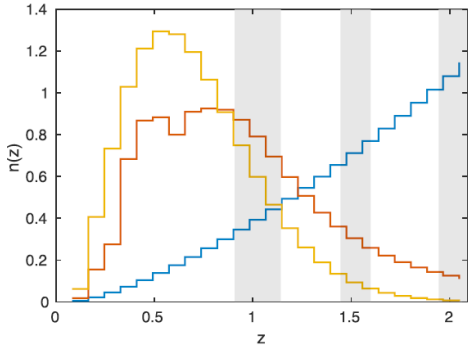

$$f(\theta_{3D})d\theta_{3D}\,d\phi = A\exp\left[-\frac{1}{2}\left(\frac{\theta_{3D}-\theta_0}{\sigma_\theta}\right)^2\right]d\theta_{3D}\times\sin(\theta_{3D})d\phi$$

From “observed” galaxy ellipticities → convergence maps → peaks

156 * (3*3 deg^2)~1400 deg^2

For comparison, we also generate no-IA samples by first randomly rotating all the galaxies to eliminate IA and then adding lensing signals

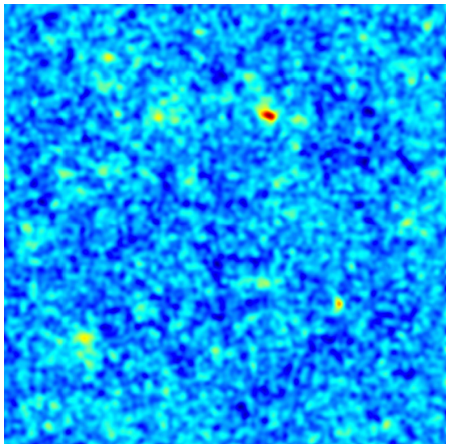

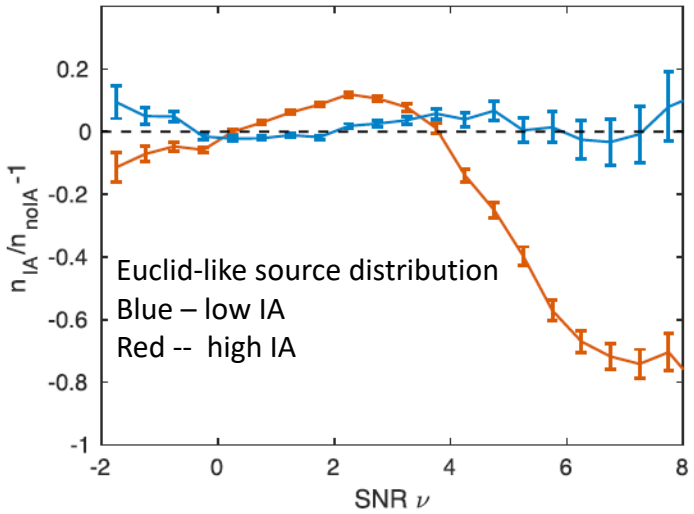

Satellite IA plays the dominant role affecting peak statistics in non-tomographic studies

How do the IA effects arise?

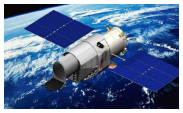

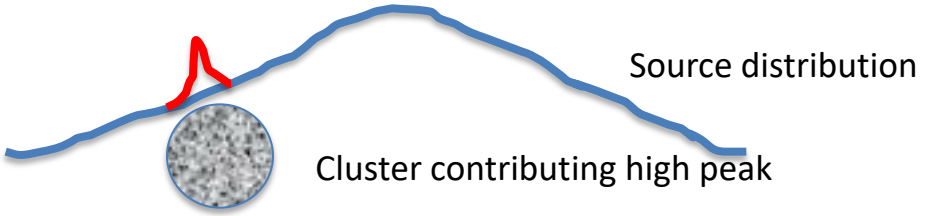

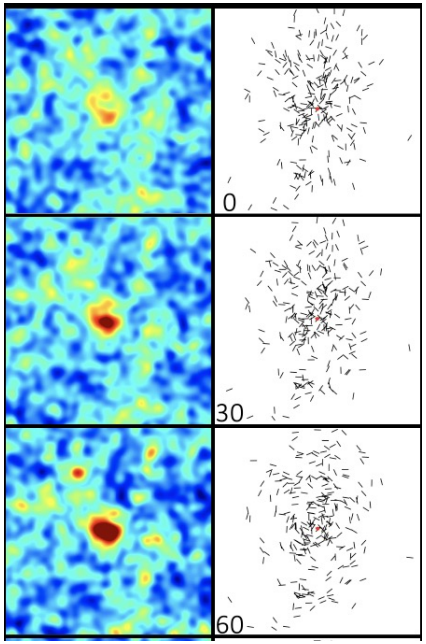

Matched peak comparison

Source sample contains cluster member galaxies

→ Affect their host cluster peak signals

→ Closely related to the dilution effect

$$\frac{\sum_{N_b}\gamma+\sum_{N_c}e}{N_b+N_c}\Big/\left(\frac{\sum_{N_b}\gamma}{N_b}\right)=\frac{N_b}{N_b+N_c}\left(1+\frac{\sum_{N_c}e}{\sum_{N_b}\gamma}\right)$$

dilution IA

High peaks are affected more significantly

For Euclid-like, ~40-20% decrease of peaks with S/N>~4 for σ_θ ~40°-80°

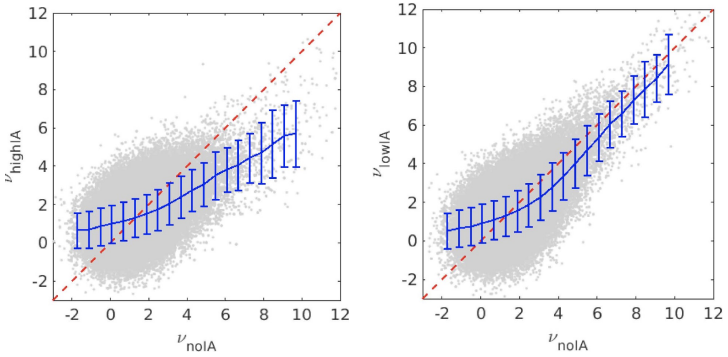

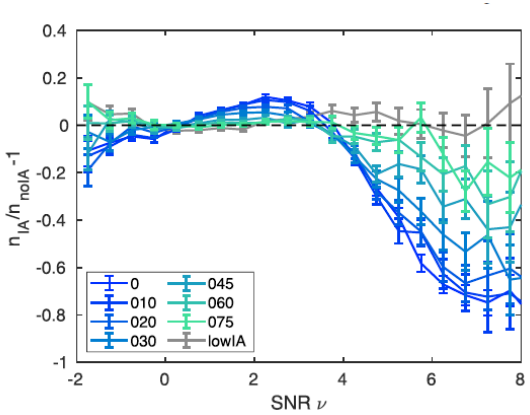

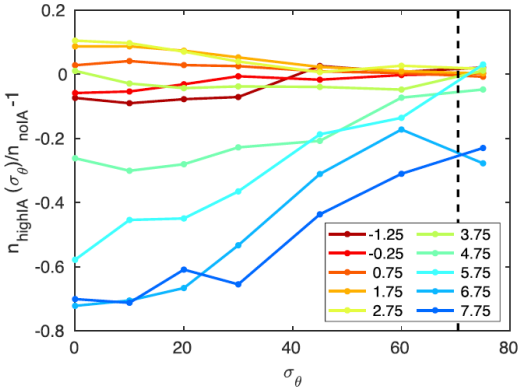

For source galaxies in narrow redshift bins

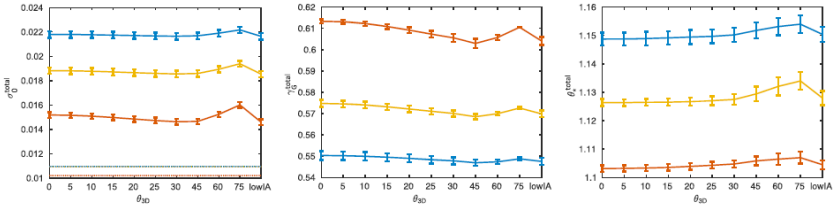

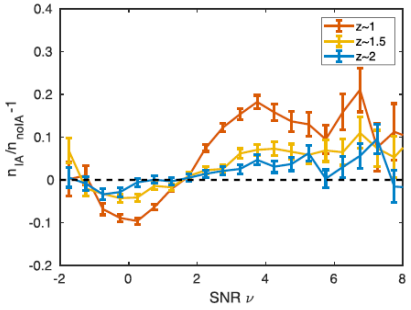

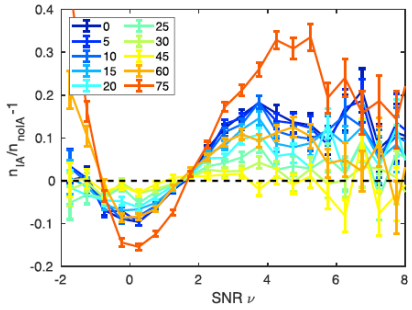

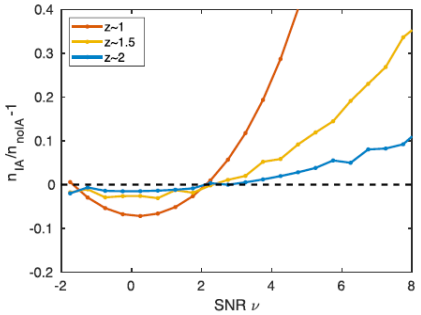

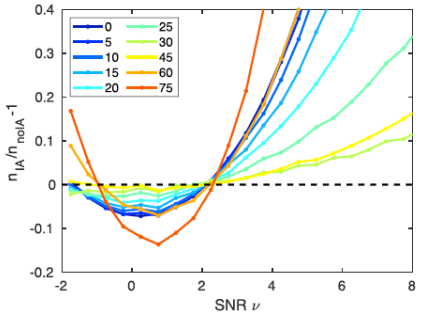

Pure Gaussian model comparisons

-- The behaviors are different: satellite IA affects cluster WL signals insignificantly because no foreground cluster members are in the source sample

-- IA contributes (both central and satellite) **additional noise** → affects peak statistics

Summary of IA effects on WL peaks

-- Decrease cluster WL signals because of their members in the shear sample

-- Change the noise properties

Incorporate IA into our model

-- reduce the cosmological bias

-- constrain IA simultaneously, particularly satellite IA

Theoretical modeling for the impact of IA on WL peaks (Zhang et al. 2025, ApJ)

Theoretical model for high peaks – Halo based (Fan et al. 2010, Yuan et al. 2018)

IA changes the lensing profile of the halos and noise properties

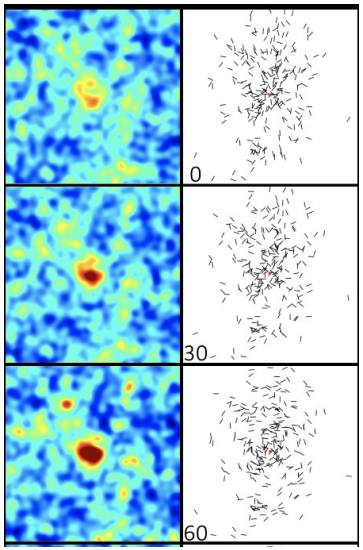

Source sample contains cluster member galaxies

$$\frac{\Sigma_{N_b}\gamma+\Sigma_{N_c}e}{N_b+N_c}\Big/\left(\frac{\Sigma_{N_b}\gamma}{N_b}\right)=\frac{N_b}{N_b+N_c}\left(1+\frac{\Sigma_{N_c}e}{\Sigma_{N_b}\gamma}\right)$$

dilution IA

Calculating the lensing profile changes

-- Estimate the member excess ratio from clusters and the source galaxy catalog considering different bins of (z, M)

-- Single halo simulations to obtain the profile change

-- Further the noise change is calculated by considering the number density change and IA

IA changes the lensing profile of the halos and the noise properties

2D Excess fraction

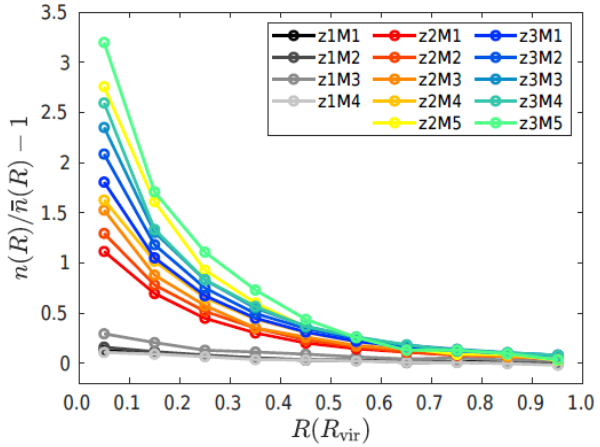

Profile change

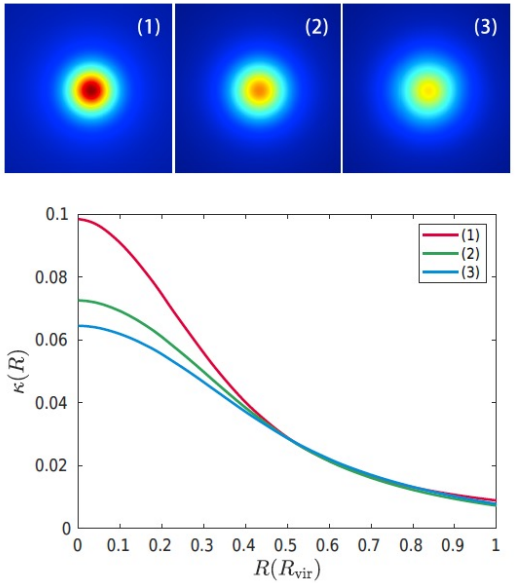

noise change

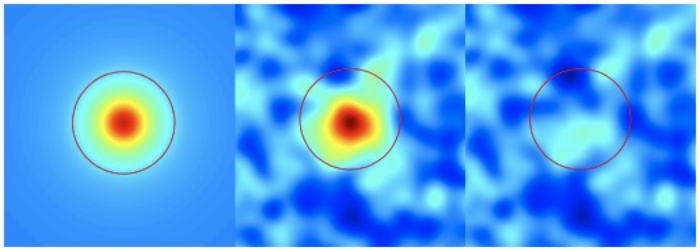

Model test at the one-halo level

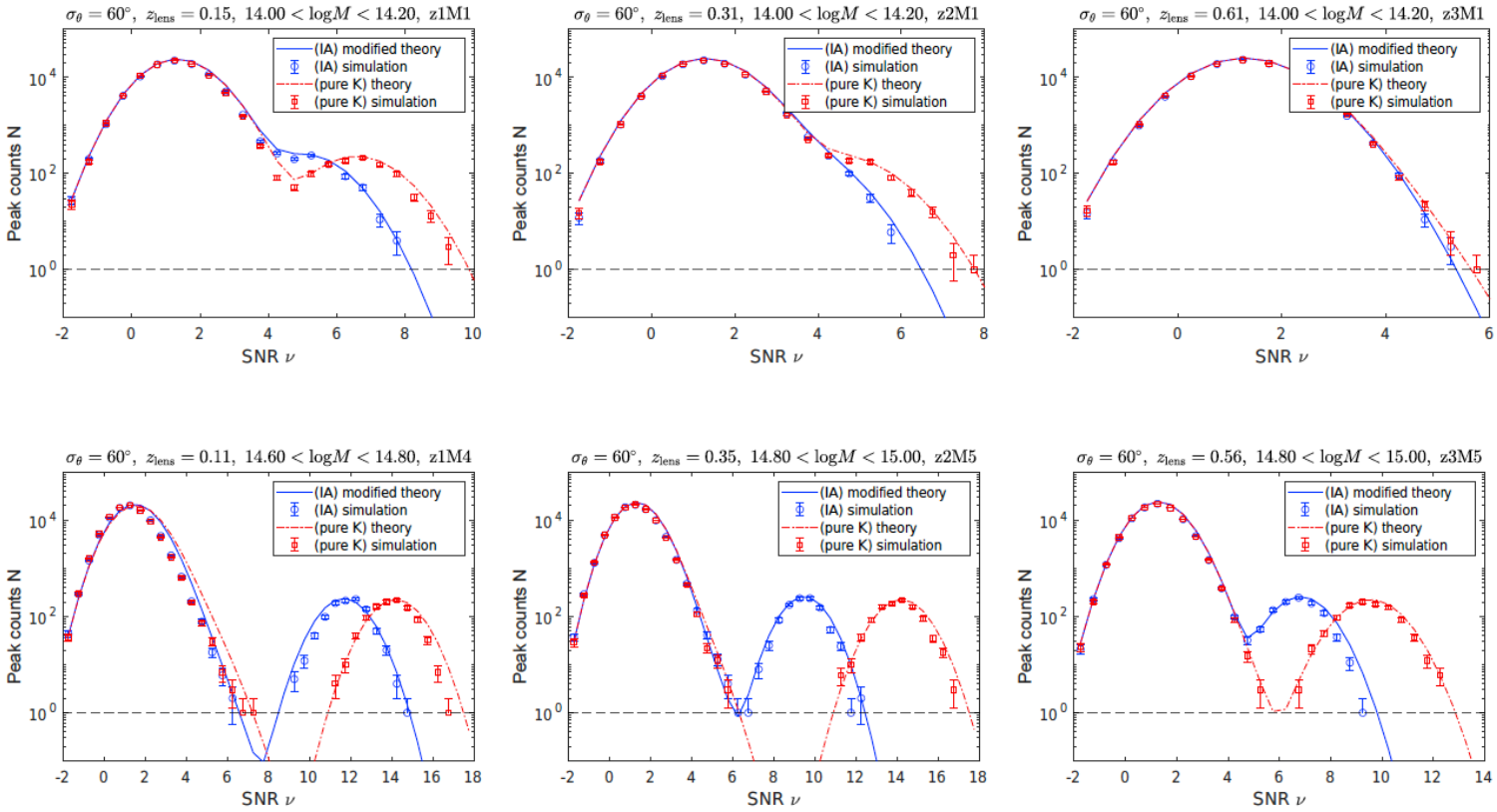

The full model test: one-halo profile and noise corrections from single halo simulations
+ large scale IA contributions to the noise

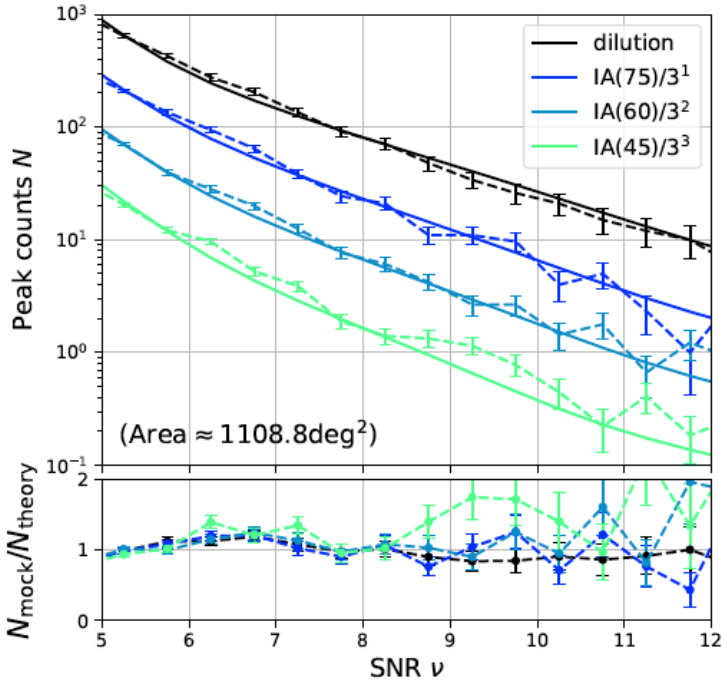

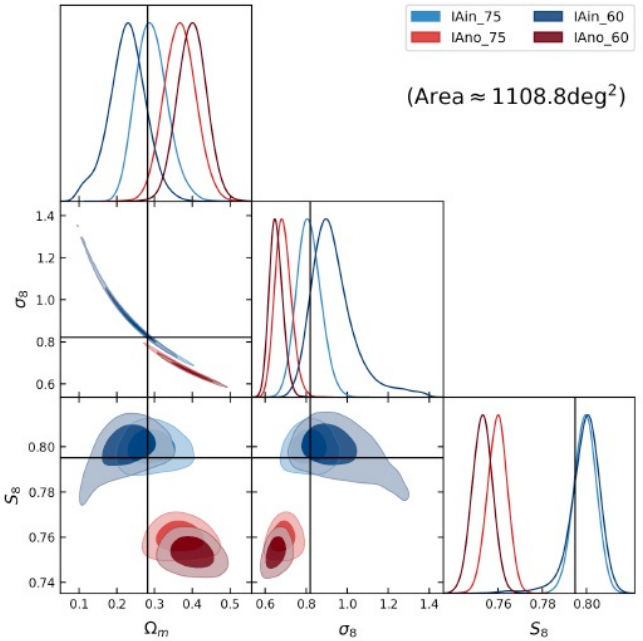

The model works well to mitigate the IA induced bias and provide a potential to probe satellite IA from WL peak analyses

Tomographic studies can help break the degeneracy between IA parameters and cosmological parameters.

- **Chinese Space Station Survey Telescope - CSST**

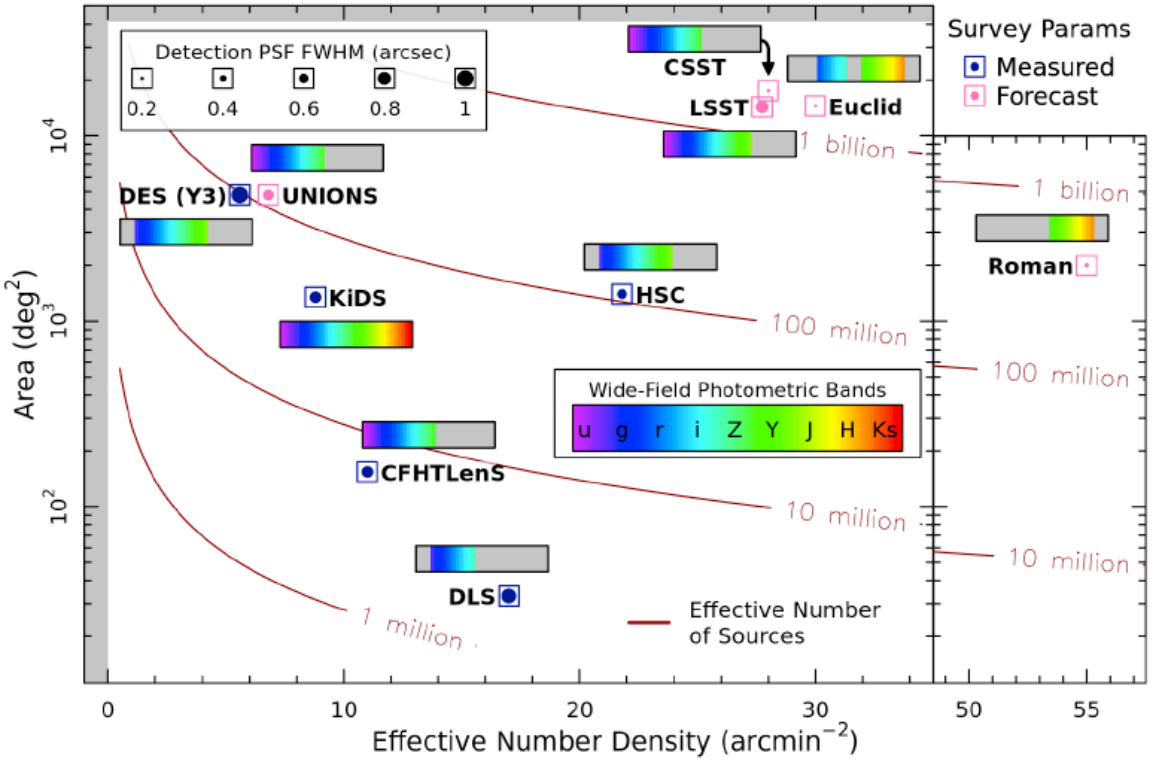

Wright, A.H. et al. 2024

Table 1 Summary of CSST instruments and surveys.

Telescope									
2 m primary, off-axis TMA, focal length = 28 m, orbit ~ 400 km, lifetime ~ 10 years									
CSST Platform									
Pointing control & Target switching	Staring accuracy/stability (3σ): 3"/0.85"@1200 s (with FGS), 9"/9"@600 s (w/o FGS); Scanning/tracking angular rate (3σ): 0.00025"~5"/s (high accuracy), 0.1'/s~1'/s (w/o FGS); Target switching duration: 1° ≯50 s, 20° ≯100 s								
Communication	20 Tb/day scientific data downlink in Ka band								
Maintenance	Performing rendezvous and docking (RVD) for on-orbit servicing at the CSS								
Primary Optical System / OTA									
Field of view (FoV)	1.72 deg² (full), 1.1 deg² (primary imaging)								
Spatial res. (point / 0th spec.)	< 0.15" / 0.3" (λ = 0.6328 μm, in 1.1 deg², 80% energy concentration region)								
Working band range	0.255 ~ 2.5 μm and Terahertz band								
Scientific Instruments									
Multi-band Imaging and Slitless Spectroscopy Survey Camera (SC)									
Primary focal plane detector	30 9k×9k CCD, 10 μm pixel/0.074", read noise ≤ 5 e⁻/pix, dark current ≤ 0.02 e⁻/(pix·s)								
Celestial calibration detector	Same as primary focal plane, read noise ≤ 10 e⁻/pix @150 kHz								
Near-IR detector	8 640×512 HgCdTe, 15 μm pixel, read noise ≤ 50 e⁻/pix @1MHz, dark current ≤ 5 e⁻/(pix·s) @80 K								
Photometric imaging:	*NUV*	*u*	*g*	*r*	*i*	*z**	*y**	*J'*	*H'*
Band (nm)	252-321	321-401	401-547	547-692	692-842	842-1080	927-1100	0.9-1.3μm	1.3-1.7 μm
Survey field	17,500 deg² wide field / 400 deg² deep field								
Exposure time (wide)	4×150 s	2×150 s	2×150 s	2×150 s	2×150 s	2×150 s	4×150 s	1×150 s	1×150 s
Exposure time (deep)	16×250 s	8×250 s	8×250 s	8×250 s	8×250 s	8×250 s	16×250 s		
Mag. limit (point, 5σ AB mag)	25.4/26.7	25.4/26.7	26.3/27.5	26.0/27.2	25.9/27.0	25.2/26.4	24.4/25.7	23.5	23.0
Slitless spectroscopy:	*GU*		*GV*		*GI**		*J'*		*H'*
Band (nm)	255-410		400-640		620-1000		0.9-1.3 μm		1.3-1.7 μm
Survey field	17,500 deg² wide field / 400 deg² deep field								
Exposure time (wide)	4×150 s		4×150 s		4×150 s		1×150 s		1×150 s
Exposure time (deep)	16×250 s		16×250 s		16×250 s				
Mag. limit (point, 5σ AB mag)	23.2 / 24.4		23.4 / 24.5		23.2 / 24.3		20.7		20.5
Spectral resolution (R)	≥ 200		≥ 200		≥ 200		≥ 100		≥ 100

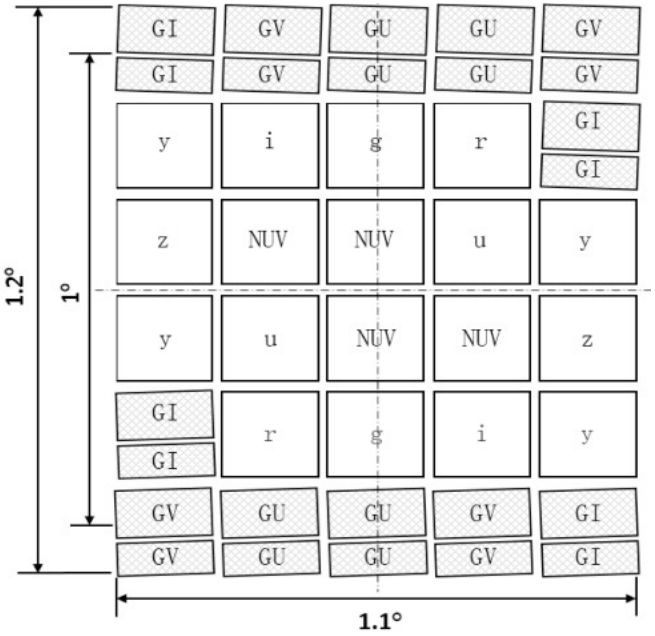

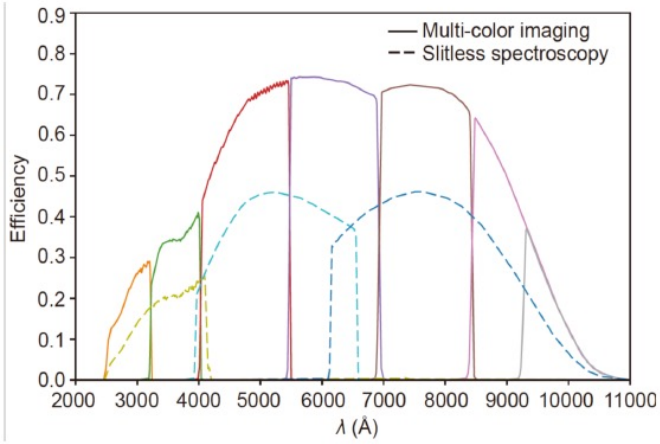

Gong et al. 2026

Sky coverage: nearly 100% overlap with Euclid

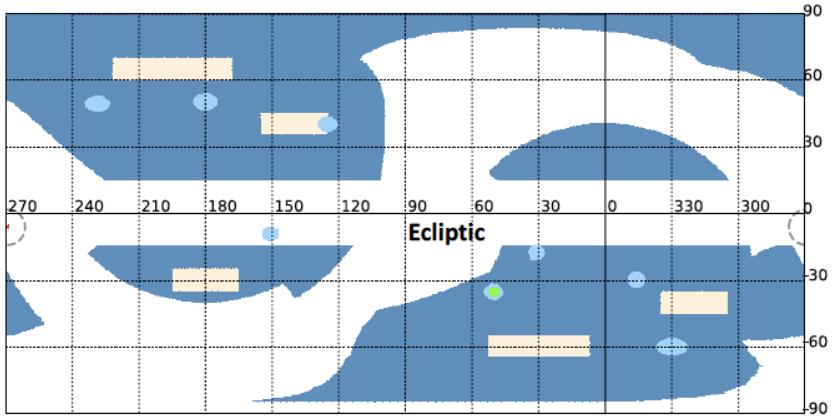

Cosmological probes: WL, galaxy clustering (photometry and slitless spectroscopy) , clusters, strong lensing, …

-- compatible with other Stage IV surveys + great complementarities

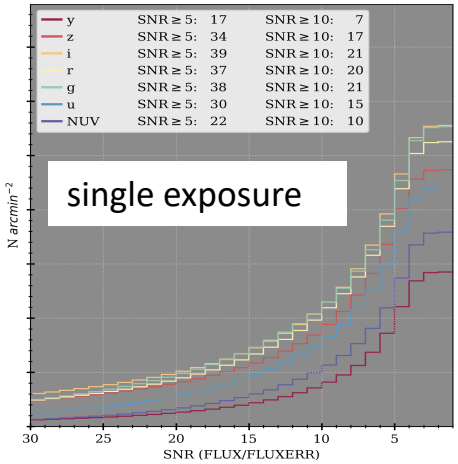

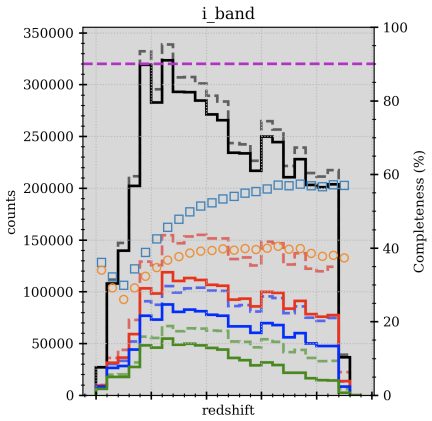

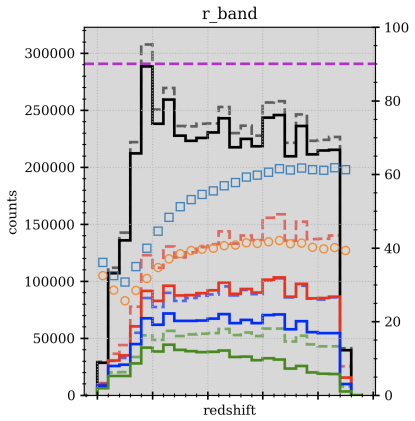

From end-to-end simulations

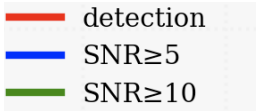

Cosmological forecast

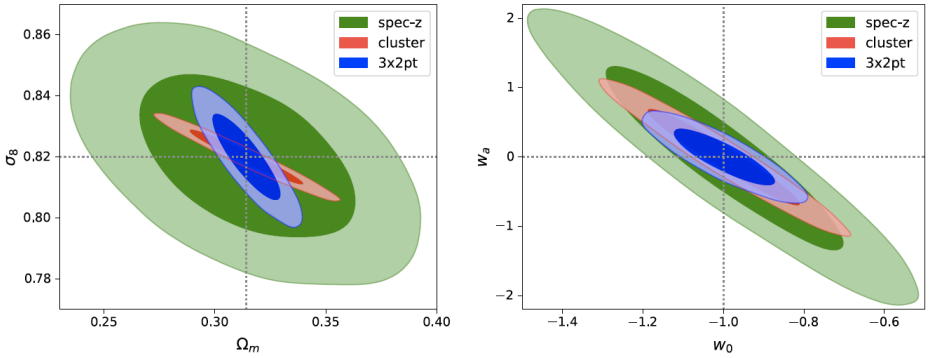

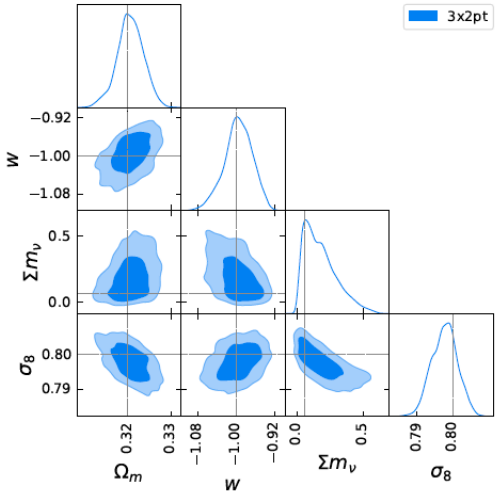

Potential synergies with Euclid (Liu,D.Z. et al. 2023)

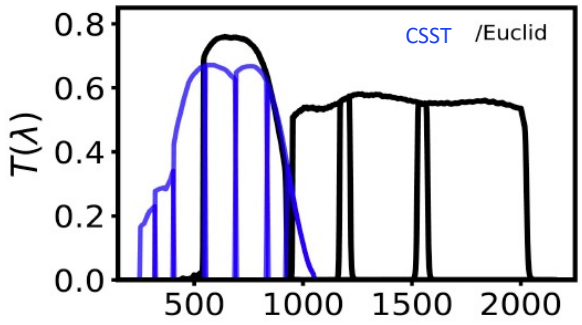

A&A 669, A128 (2023)
https://doi.org/10.1051/0004-6361/202243978
© D. Z. Liu et al. 2023

Astronomy & Astrophysics

Potential scientific synergies in weak lensing studies between the CSST and *Euclid* space probes

D. Z. Liu[1], X. M. Meng[2], X. Z. Er[1], Z. H. Fan[1], M. Kilbinger[3], G. L. Li[4,5], R. Li[6,7,8], T. Schrabback[9,10], D. Scognamiglio[9], H. Y. Shan[11,12], C. Tao[13], Y. S. Ting[14,15], J. Zhang[16], S. H. Cheng[17], S. Farrens[3], L. P. Fu[18], H. Hildebrandt[19], X. Kang[4,5], J. P. Kneib[20,21], X. K. Liu[1], Y. Mellier[22,23], R. Nakajima[9], P. Schneider[9], J. L. Starck[3], C. L. Wei[4], A. H. Wright[19], and H. Zhan[2,24]

(Affiliations can be found after the references)

Received 9 May 2022 / Accepted 28 October 2022

ABSTRACT

Aims. With the next generation of large surveys poised to join the ranks of observational cosmology in the near future, it is important to explore their potential synergies and to maximize their scientific outcomes. In this study, we aim to investigate the complementarity of two upcoming space missions: *Euclid* and the China Space Station Telescope (CSST), both of which will be focused on weak gravitational lensing for cosmology. In particular, we analyze the photometric redshift (photo-*z*) measurements by combining NUV, *u*, *g*, *r*, *i*, *z*, *y* bands from CSST with the VIS, *Y*, *J*, *H* bands from *Euclid*, and other optical bands from the ground-based *Vera C. Rubin* Observatory Legacy Survey of Space and Time (LSST) and Dark Energy Survey. We also consider the advantages of combining the two space observational data in simplifying image deblending. For *Euclid*, weak lensing measurements use the broad optical wavelength range of 550–900 nm, for which chromatic point-spread function (PSF) effects are significant. For this purpose, the CSST narrow-band data in the optical can provide valuable information for *Euclid* to obtain more accurate PSF measurements and to calibrate the color and color-gradient biases for galaxy shear measurements.

Methods. We created image simulations, using the *Hubble* Deep UV data as the input catalog, for different surveys and quantified the photo-*z* performance using the EAZY template fitting code. For the blending analyses, we employed high-resolution HST-ACS CANDELS *F606W* and *F814W* data to synthesize mock simulated data for *Euclid*, CSST, and an LSST-like survey. We analyzed the blending fraction for different cases as well as the blending effects on galaxy photometric measurements. Furthermore, we demonstrated that CSST can provide a large enough number of high signal-to-noise ratio multi-band galaxy images to calibrate the color-gradient biases for *Euclid*.

Results. The sky coverage of *Euclid* lies entirely within the CSST footprint. The combination of *Euclid* with the CSST data can thus be done more uniformly than with the various ground-based data that are part of the *Euclid* survey. Our studies show that by combining *Euclid* and CSST, we can reach a photo-*z* precision of $\sigma_{\rm MAD} \approx 0.04$ and an outlier fraction of $\eta \approx 2.4\%$ at the nominal depth of the *Euclid* Wide Survey (VIS < 24.5 AB mag). For CSST, including the *Euclid Y*, *J*, *H* bands reduces the overall photo-*z* outlier fraction from ~8.5% to 2.4%. For $z > 1$, the improvements are even more significant. Because of the similarly high resolutions, the data combination of *Euclid* and CSST can be relatively straightforward for photometry measurements. On the other hand, to include ground-based data, sophisticated deblending utilizing priors from high-resolution space observations are required. The multi-band data from CSST are very helpful in controlling the chromatic PSF effect for *Euclid* VIS shear measurements. The color-gradient bias for *Euclid* galaxies with different bulge-to-total flux ratio at different redshifts can be well calibrated to the level of 0.1% using galaxies from the CSST deep survey.

Key words. dark energy – dark matter – gravitational lensing: weak – large-scale structure of Universe – surveys – telescopes

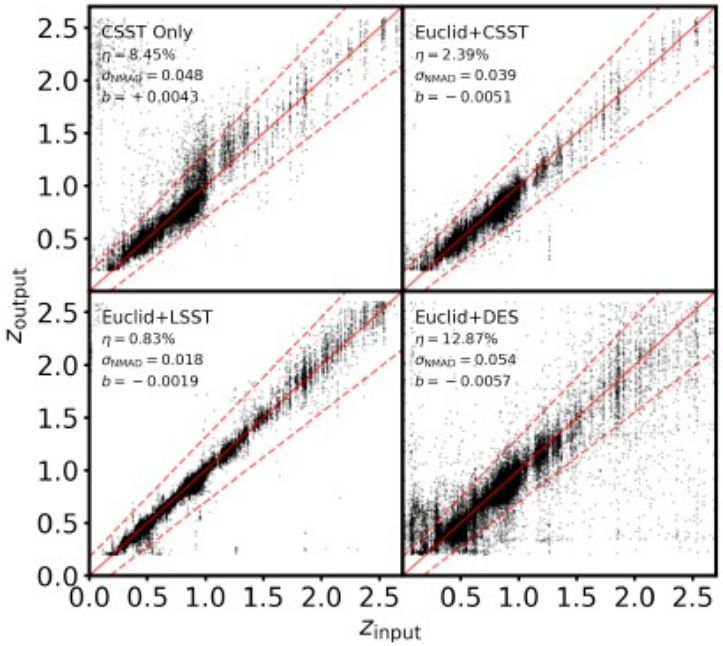

Table 2. Photo-z statistics in different cases.

Combination	Bias	$\sigma_{\rm NMAD}$	η
CSST-only	+0.0043	0.048	8.45%
Euclid+CSST	−0.0051	0.039	2.39%
Euclid+LSST-like	−0.0019	0.018	0.83%
Euclid+DES-like	−0.0057	0.054	12.87%

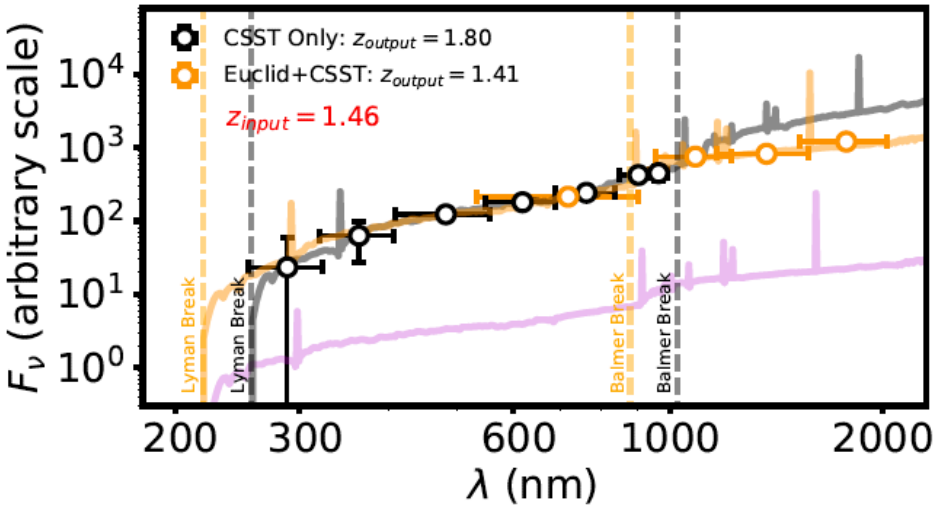

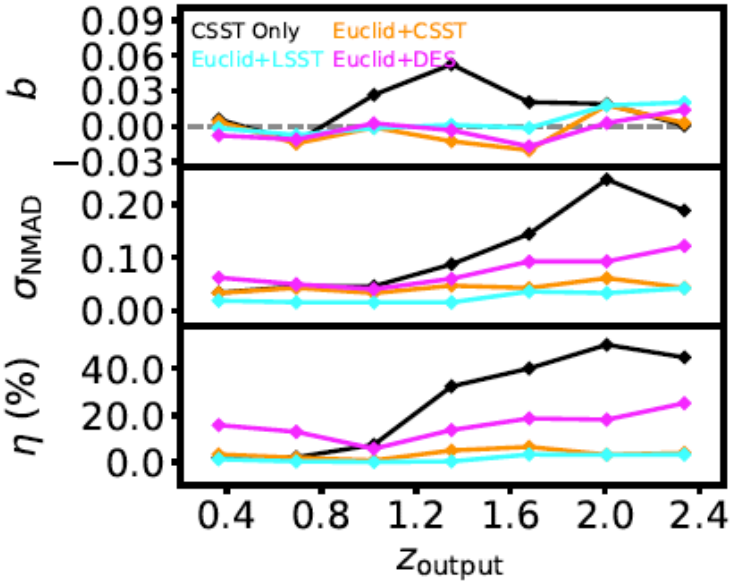

Blending problem: With the increase of depth, the problem of galaxy blending becomes increasingly troublesome, particularly for ground-based observations

→ Combining data from CSST and Euclid would be more straightforward than combining ground-based data and Euclid; also can be done uniformly over the whole survey areas.

Blending fraction

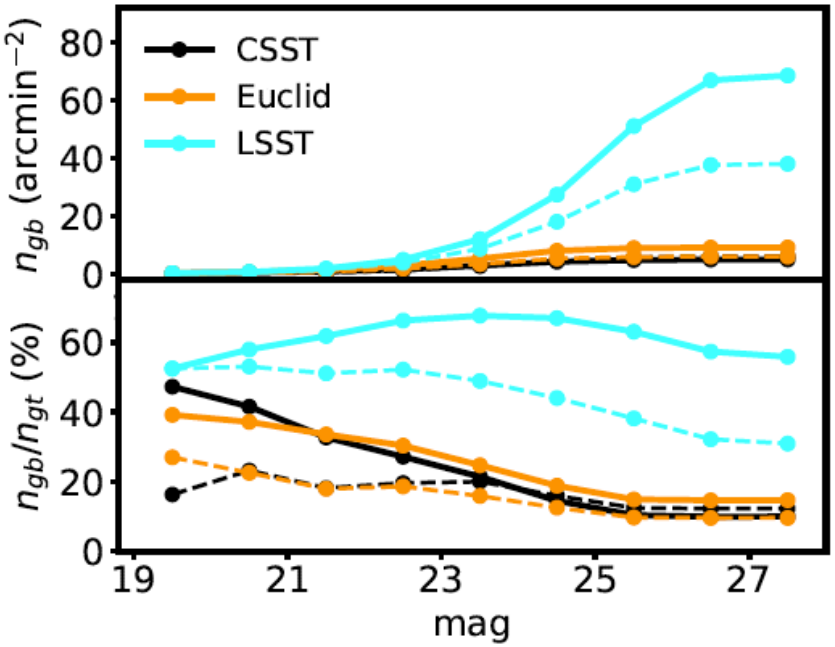

Total blends

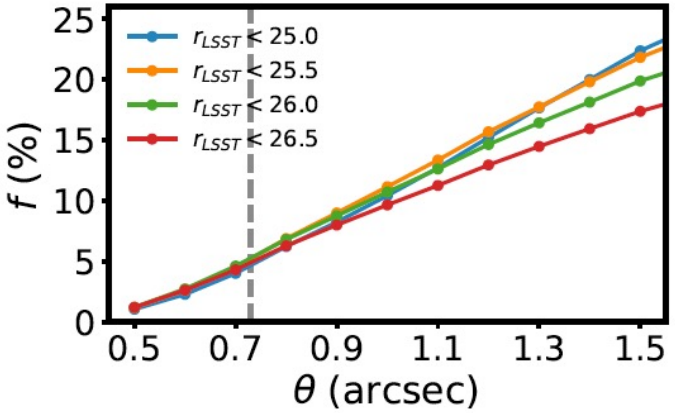

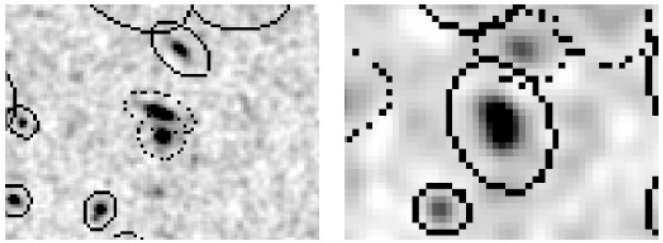

PSF chromaticity

-- PSF is wavelength dependent

-- stars and galaxies have different SEDs

-- the extrapolation of PSF measured from stars to galaxies can have biases, especially for Euclid with the broad VIS band

-- galaxies have color gradients → additional biases

CSST can provide enough number of high S/N >50 narrower bands data for Euclid calibration

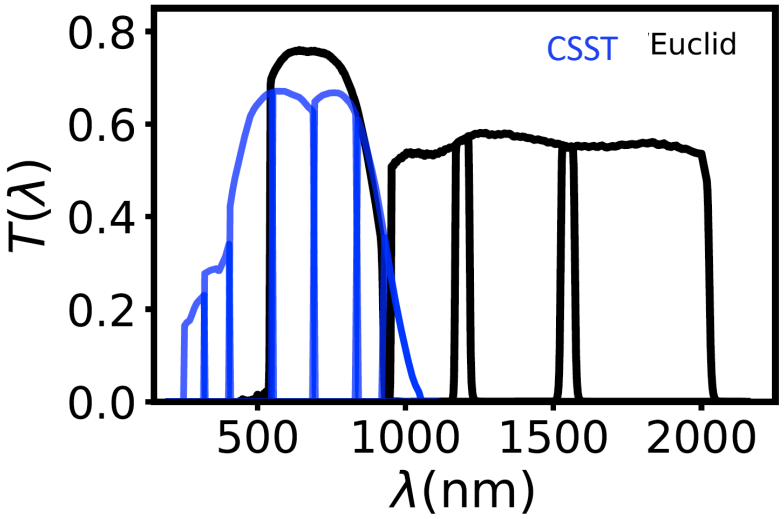

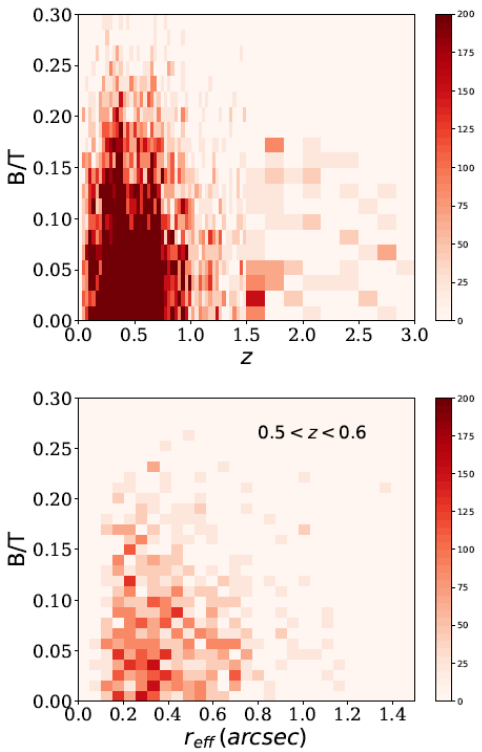

• Summary

- With the upcoming Stage IV surveys, non-Gaussian statistical analyses are crucially important
- Peak steepness analyses provide added value
  – sensitive to halo density profile, which encodes important astrophysical and physical info.
- Understanding different systematics are critical
- Synergetic studies between different Stage IV surveys can be greatly beneficial

Thank you